ForLion: A New Algorithm for D-optimal Designs under General Parametric Statistical Models with Mixed Factors

Yifei Huang[1], Keren Li[2],
Abhyuday Mandal[3], and Jie Yang[1]

[1]University of Illinois at Chicago,
[2]University of Alabama at Birmingham, and
[3]University of Georgia

December 19, 2023

Abstract

In this paper, we address the problem of designing an experiment with both discrete and continuous factors under fairly general parametric statistical models. We propose a new algorithm, named ForLion, to search for optimal designs under the D-criterion. The algorithm performs an exhaustive search in a design space with mixed factors while keeping high efficiency and reducing the number of distinct experimental settings. Its optimality is guaranteed by the general equivalence theorem. We demonstrate its superiority over state-of-the-art design algorithms using real-life experiments under multinomial logistic models (MLM) and generalized linear models (GLM). Our simulation studies show that the ForLion algorithm could reduce the number of experimental settings by 25% or improve the relative efficiency of the designs by 17.5% on average. Our algorithm can help the experimenters reduce the time cost, the usage of experimental devices, and thus the total cost of their experiments while preserving high efficiencies of the designs.

Key words and phrases: ForLion algorithm, Generalized linear model, Lift-one algorithm, Mixed factors, Multinomial logistic model, D-optimal design

1. Introduction

Our research is motivated by an experiment on the emergence of house flies for studying biological controls of disease-transmitting fly species (Itepan, 1995; Zocchi and Atkinson, 1999). In the original experiment (Itepan, 1995), $n = 3,500$ pupae were grouped evenly into seven subsets and exposed in a radiation device to seven different gamma radiation levels $x_i \in \{80, 100, 120, 140, 160, 180, 200\}$ in units Gy, respectively. After a certain period of time, each pupa had one of three possible outcomes: `unopened`, `opened but died` (before completing emergence), or `completed emergence`. The total experimental costs

in time and expense were closely related to the number of distinct settings of the radiation device. By searching the grid-1 settings in $[80, 200]$ using their lift-one algorithm, Bu et al. (2020) proposed a design on five settings $\{80, 122, 123, 157, 158\}$ and improved the relative efficiency of the original design by 20.8% in terms of D-criterion. More recently, Ai et al. (2023) obtained a design focusing on four settings $\{0, 101.1, 147.8, 149.3\}$ by employing an algorithm that combines the Fedorov-Wynn (Fedorov and Leonov, 2014) and lift-one (Bu et al., 2020) algorithms on searching the continuous region $[0, 200]$. Having noticed that both Bu et al. (2020)'s and Ai et al. (2023)'s designs contain pairs of settings that are close to each other, we propose a new algorithm, called the ForLion algorithm (see Section 2), that incorporates a merging step to combine close experimental settings while maintaining a high relative efficiency. For this case, our proposed algorithm identifies a D-optimal design on $\{0, 103.56, 149.26\}$, which may lead to a 40% or 25% reduction of the experimental cost compared to Bu et al. (2020)'s or Ai et al. (2023)'s design, respectively.

In this paper, we consider experiments under a fairly general statistical model with mixed factors. The pre-determined design region $\mathcal{X} \subset \mathbb{R}^d$ with $d \geq 1$ factors is compact, that is, bounded and closed, for typical applications (see Section 2.4 in Fedorov and Leonov (2014)). For many applications, $\mathcal{X} = \prod_{j=1}^{d} I_j$, where I_j is either a finite set of levels for a qualitative or discrete factor, or an interval $[a_j, b_j]$ for a quantitative or continuous factor. To simplify the notations, we assume that the first k factors are continuous, where $0 \leq k \leq d$, and the last $d - k$ factors are discrete. Suppose $m \geq 2$ distinct experimental settings $\mathbf{x}_1, \ldots, \mathbf{x}_m \in \mathcal{X}$, known as the *design points*, are chosen, and $n > 0$ experimental units are available for the experiment with $n_i \geq 0$ subjects allocated to $\mathbf{x}_i$ with $n = \sum_{i=1}^{m} n_i$. We assume that the responses, which could be vectors, are independent and follow a parametric model $M(\mathbf{x}_i; \boldsymbol{\theta})$ with some unknown parameter(s) $\boldsymbol{\theta} \in \mathbb{R}^p$, $p \geq 1$. In the design theory, $\mathbf{w} = (w_1, \ldots, w_m)^T = (n_1/n, \ldots, n_m/n)^T$, known as an *approximate allocation*, is often considered instead of the *exact allocation* $\mathbf{n} = (n_1, \ldots, n_m)^T$. Under regularity conditions, the corresponding Fisher information matrix is $\mathbf{F} = \sum_{i=1}^{m} w_i \mathbf{F}_{\mathbf{x}_i} \in \mathbb{R}^{p \times p}$ up to a constant n, where $\mathbf{F}_{\mathbf{x}_i}$ is the Fisher information at $\mathbf{x}_i$. In this paper, the design under consideration takes the form of $\boldsymbol{\xi} = \{(\mathbf{x}_i, w_i), i = 1, \ldots, m\}$, where m is a flexible positive integer, $\mathbf{x}_1, \ldots, \mathbf{x}_m$ are distinct design points from $\mathcal{X}$, $0 \leq w_i \leq 1$, and $\sum_{i=1}^{m} w_i = 1$. We also denote $\boldsymbol{\Xi} = \{\{(\mathbf{x}_i, w_i), i = 1, \ldots, m\} \mid m \geq 1; \mathbf{x}_i \in \mathcal{X}, 0 \leq w_i \leq 1, i = 1, \ldots, m; \sum_{i=1}^{m} w_i = 1\}$ be the collection of all feasible designs.

Under different criteria, such as D-, A-, or E-criterion (see, for example, Chapter 10 in Atkinson et al. (2007)), many numerical algorithms have been proposed for finding optimal designs. If all factors are discrete, the design region $\mathcal{X}$ typically contains a finite number of design points, still denoted by m. Then the design problem is to optimize the approximate allocation $\mathbf{w} = (w_1, \ldots, w_m)^T$. Commonly used design algorithms include Fedorov-Wynn (Fedorov, 1972; Fedorov and Hackl, 1997), multiplicative (Titterington, 1976, 1978; Silvey et al., 1978), cocktail (Yu, 2011), and lift-one (Yang and Mandal, 2015; Yang et al., 2017; Bu et al., 2020), etc. Besides, classical optimization techniques such as Nelder-Mead, quasi-Newton, conjugate-gradient, and simulated annealing may also be used for the same purpose (Nocedal and Wright, 1999). Among them, the lift-one algorithm runs faster and ends with fewer design points (Yang et al., 2016).

When the factors are continuous, the Fedorov-Wynn algorithm can still be used by adding a new design point in each iteration, which maximizes a sensitivity function on $\mathcal{X}$ (Fedorov and Leonov, 2014). To improve the efficiency, Ai et al. (2023) proposed a new algorithm for D-optimal designs under a continuation-ratio link model with continuous factors, which essentially incorporates the Fedorov-Wynn (for adding new design points) and lift-one (for optimizing the approximate allocation) algorithms. Nevertheless, the Fedorov-Wynn step tends to add unnecessary closely-spaced design points (see Section 3.2), which may increase the experimental cost. An alternative approach is to discretize the continuous factors and consider only the grid points (Yang et al., 2013), which may be computationally expensive especially when the number of factors is moderate or large.

Little has been done to construct efficient designs with mixed factors. Lukemire et al. (2019) proposed the d-QPSO algorithm, a modified quantum-behaved particle swarm optimization (PSO) algorithm, for D-optimal designs under generalized linear models with binary responses. Later, Lukemire et al. (2022) extended the PSO algorithm for locally D-optimal designs under the cumulative logit model with ordinal responses. However, like other stochastic optimization algorithms, the PSO-type algorithms cannot guarantee an optimal solution will ever be found (Kennedy and Eberhart, 1995; Poli et al., 2007).

Following Ai et al. (2023) and Lukemire et al. (2019, 2022), we choose D-criterion, which maximizes the objective function $f(\boldsymbol{\xi}) = |\sum_{i=1}^{m} w_i \mathbf{F}_{\mathbf{x}_i}|$, $\boldsymbol{\xi} \in \boldsymbol{\Xi}$. Throughout this paper, we assume $f(\boldsymbol{\xi}) > 0$ for some $\boldsymbol{\xi} \in \boldsymbol{\Xi}$ to avoid trivial optimization problems. Unlike Bu et al. (2020) and Ai et al. (2023), the proposed ForLion algorithm does not need to assume $\text{rank}(\mathbf{F}_{\mathbf{x}}) < p$ for all $\mathbf{x} \in \mathcal{X}$ (see Remark 1 and Example 1). Compared with the PSO-type algorithms for similar purposes (Lukemire et al., 2019, 2022), our ForLion algorithm could improve the relative efficiency of the designs significantly (see Example 3 for an electrostatic discharge experiment discussed by Lukemire et al. (2019) and Section S.6 of the Supplementary Material for a surface defects experiment (Phadke, 1989; Wu, 2008; Lukemire et al., 2022)).

The remaining parts of this paper are organized as follows. In Section 2, we present the ForLion algorithm for general parametric statistical models. In Section 3, we derive the theoretical results for multinomial logistic models (MLM) and revisit the motivated example to demonstrate our algorithm's performance with mixed factors under general parametric models. In Section 4, we specialize our algorithm for generalized linear models (GLM) to enhance computational efficiency by using model-specified formulae and iterations. We use simulation studies to show the advantages of our algorithm. We conclude in Section 5.

2.   ForLion for D-optimal designs with mixed factors

In this section, we propose a new algorithm, called the *ForLion* (<u>F</u>irst-<u>or</u>der <u>L</u>ift-<u>one</u>) algorithm, for constructing D-optimal designs under a general parametric model $M(\mathbf{x}; \boldsymbol{\theta})$ with $\mathbf{x} \in \mathcal{X} \subset \mathbb{R}^d$, $d \geq 1$. As mentioned earlier, the design region $\mathcal{X} = \prod_{j=1}^{d} I_j$, where $I_j = [a_j, b_j]$ for $1 \leq j \leq k$, $-\infty < a_j < b_j < \infty$, and I_j is a finite set of at

least two distinct numerical levels for $j > k$. In order to simplify the notations, we still denote $a_j = \min I_j$ and $b_j = \max I_j$ even if I_j is a finite set. In this paper, we assume $1 \leq k \leq d$. That is, there is at least one continuous factor. The goal is to find a design $\boldsymbol{\xi} = \{(\mathbf{x}_i, w_i), i = 1, \ldots, m\} \in \boldsymbol{\Xi}$ maximizing $f(\boldsymbol{\xi}) = |\mathbf{F}(\boldsymbol{\xi})|$, the determinant of $\mathbf{F}(\boldsymbol{\xi})$, where $\mathbf{F}(\boldsymbol{\xi}) = \sum_{i=1}^{m} w_i \mathbf{F}_{\mathbf{x}_i} \in \mathbb{R}^{p \times p}$. Here $m \geq 1$ is flexible.

Algorithm 1. ForLion

  $0°$ Set up tuning parameters $\delta > 0$ as the merging threshold and $\epsilon > 0$ as the converging threshold. For example, $\delta = 10^{-6}$ and $\epsilon = 10^{-12}$.

  $1°$ Construct an initial design $\boldsymbol{\xi}_0 = \{(\mathbf{x}_i^{(0)}, w_i^{(0)}), i = 1, \ldots, m_0\}$ such that (i) $\|\mathbf{x}_i^{(0)} - \mathbf{x}_j^{(0)}\| \geq \delta$ for any $i \neq j$; and (ii) $|\mathbf{F}(\boldsymbol{\xi}_0)| > 0$. For example, one may sequentially and randomly choose $\mathbf{x}_i^{(0)}$ from either $\prod_{j=1}^{d}\{a_j, b_j\}$ or $\prod_{j=1}^{d} I_j$ such that the new point is at least δ away from the previous points, until some m_0 such that $|\sum_{i=1}^{m_0} \mathbf{F}_{\mathbf{x}_i^{(0)}}| > 0$. The weights $w_i^{(0)}$ may be defined uniformly (all equal to $1/m_0$) or randomly (proportional to U_i with U_i's i.i.d. from an exponential distribution).

  $2°$ Merging step: Given the design $\boldsymbol{\xi}_t = \{(\mathbf{x}_i^{(t)}, w_i^{(t)}), i = 1, \ldots, m_t\}$ at the tth iteration, check the pairwise Euclidean distances among $\mathbf{x}_i^{(t)}$'s. If there exist $1 \leq i < j \leq m_t$, such that, $\|\mathbf{x}_i^{(t)} - \mathbf{x}_j^{(t)}\| < \delta$, then merge the two points into a new point $(\mathbf{x}_i^{(t)} + \mathbf{x}_j^{(t)})/2$ with weight $w_i^{(t)} + w_j^{(t)}$, and replace m_t by $m_t - 1$. Repeat the procedure till any two remaining points have a distance at least δ.

  $3°$ Lift-one step: Given $\boldsymbol{\xi}_t$, run the lift-one algorithm (see Remark 1) with converging threshold ϵ to find the converged allocation $w_1^*, \ldots, w_{m_t}^*$ for the design points $\mathbf{x}_1^{(t)}, \ldots, \mathbf{x}_{m_t}^{(t)}$. Replace $w_i^{(t)}$'s with w_i^*'s, respectively.

  $4°$ Deleting step: Update $\boldsymbol{\xi}_t$ by removing all $\mathbf{x}_i^{(t)}$'s that have $w_i^{(t)} = 0$.

  $5°$ New point step: Given $\boldsymbol{\xi}_t$, find a point $\mathbf{x}^* = (x_1^*, \ldots, x_d^*)^T \in \mathcal{X}$ that maximizes $d(\mathbf{x}, \boldsymbol{\xi}_t) = \mathrm{tr}(\mathbf{F}(\boldsymbol{\xi}_t)^{-1}\mathbf{F}_{\mathbf{x}})$. Recall that the first k factors are continuous. If $1 \leq k < d$, we denote $\mathbf{x}_{(1)} = (x_1, \ldots, x_k)^T$ and $\mathbf{x}_{(2)} = (x_{k+1}, \ldots, x_d)^T$. Then $\mathbf{x} = (\mathbf{x}_{(1)}^T, \mathbf{x}_{(2)}^T)^T$. Fixing each $\mathbf{x}_{(2)} \in \prod_{j=k+1}^{d} I_j$, we use the "L-BFGS-B" quasi-Newton method (Byrd et al., 1995) to find

$$\mathbf{x}_{(1)}^* = \mathrm{argmax}_{\mathbf{x}_{(1)} \in \prod_{i=1}^{k}[a_i, b_i]} d((\mathbf{x}_{(1)}^T, \mathbf{x}_{(2)}^T)^T, \boldsymbol{\xi}_t)$$

  Note that $\mathbf{x}_{(1)}^*$ depends on $\mathbf{x}_{(2)}$. Then $\mathbf{x}^*$ is obtained by finding the $\mathbf{x}_{(2)}^*$ associated with the largest $d(((\mathbf{x}_{(1)}^*)^T, \mathbf{x}_{(2)}^T)^T, \boldsymbol{\xi}_t)$. If $k = d$, that is, all factors are continuous, we can always find $\mathbf{x}^* = \mathrm{argmax}_{\mathbf{x} \in \mathcal{X}} d(\mathbf{x}, \boldsymbol{\xi}_t)$ directly.

  $6°$ If $d(\mathbf{x}^*, \boldsymbol{\xi}_t) \leq p$, go to Step $7°$. Otherwise, we let $\boldsymbol{\xi}_{t+1} = \boldsymbol{\xi}_t \bigcup \{(\mathbf{x}^*, 0)\}$, replace t by $t + 1$, and go back to Step $2°$.

  $7°$ Report $\boldsymbol{\xi}_t$ as the D-optimal design.

Given a design $\boldsymbol{\xi} = \{(\mathbf{x}_i, w_i), i = 1, \ldots, m\}$ reported by the ForLion algorithm, the general equivalence theorem (Kiefer, 1974; Pukelsheim, 1993; Stufken and Yang, 2012; Fedorov and Leonov, 2014) guarantees its D-optimality on $\mathcal{X}$. As a direct conclusion of Theorem 2.2 in Fedorov and Leonov (2014), we have the theorem as follows under the regularity conditions (see Assumptions (A1), (A2) and (B1) $\sim$ (B4) in Section 2.4 of Fedorov and Leonov (2014)):

Theorem 1. *Under regularity conditions, there exists a D-optimal design that contains no more than $p(p + 1)/2$ design points. Furthermore, if $\boldsymbol{\xi}$ is obtained by Algorithm 1, it must be D-optimal.*

We relegate the proof of Theorem 1 and others to Section S.11 of the Supplementary Material.

Remark 1. Lift-one step for general parametric models: For commonly used parametric models, $\mathrm{rank}(\mathbf{F_x}) < p$ for each $\mathbf{x} \in \mathcal{X}$. For example, all GLMs satisfy $\mathrm{rank}(\mathbf{F_x}) = 1$ (see Section 4). However, there exist special cases that $\mathrm{rank}(\mathbf{F_x}) = p$ for almost all $\mathbf{x} \in \mathcal{X}$ (see Example 1 in Section 3.1).

The original lift-one algorithm (see Algorithm 3 in the Supplementary Material of Huang et al. (2023)) requires $0 \le w_i < 1$ for all $i = 1, \dots, m$ given the current allocation $\mathbf{w} = (w_1, \dots, w_m)^T$. If $\mathrm{rank}(\mathbf{F}_{\mathbf{x}_i}) < p$ for all i, then $f(\boldsymbol{\xi}) > 0$ implies $0 \le w_i < 1$ for all i. In that case, same as in the original lift-one algorithm, we define the allocation function as

$$\mathbf{w}_i(z) = \left(\frac{1-z}{1-w_i}w_1, \dots, \frac{1-z}{1-w_i}w_{i-1}, z, \frac{1-z}{1-w_i}w_{i+1}, \dots, \frac{1-z}{1-w_i}w_m \right)^T = \frac{1-z}{1-w_i}\mathbf{w} + \frac{z-w_i}{1-w_i}\mathbf{e}_i$$

where $\mathbf{e}_i = (0, \dots, 0, 1, 0, \dots, 0)^T \in \mathbb{R}^m$ whose ith coordinate is 1. However, if $\mathrm{rank}(\mathbf{F}_{\mathbf{x}_i}) = p$ and $w_i = 1$ for some i, we still have $f(\boldsymbol{\xi}) > 0$ but the above $\mathbf{w}_i(z)$ is not well defined. In that case, we define the allocation function in the ForLion algorithm as

$$\mathbf{w}_i(z) = \left(\frac{1-z}{m-1}, \dots, \frac{1-z}{m-1}, z, \frac{1-z}{m-1}, \dots, \frac{1-z}{m-1} \right)^T = \frac{m(1-z)}{m-1}\mathbf{w}_u + \frac{zm-1}{m-1}\mathbf{e}_i$$

where $\mathbf{w}_u = (1/m, \dots, 1/m)^T \in \mathbb{R}^m$ is a uniform allocation. For $j \ne i$, we define $\mathbf{w}_j(z) = (1-z)\mathbf{e}_i + z\mathbf{e}_j$. The rest parts are the same as the original life-one algorithm. □

Remark 2. Convergence in finite iterations: In practice, we may relax the stopping rule $d(\mathbf{x}^*, \boldsymbol{\xi}_t) \le p$ in Step 6° of Algorithm 1 to $d(\mathbf{x}^*, \boldsymbol{\xi}_t) \le p + \epsilon$, where ϵ could be the same as in Step 0°. By Section 2.5 in Fedorov and Leonov (2014), $f((1-\alpha)\boldsymbol{\xi}_t + \alpha\mathbf{x}^*) - f(\boldsymbol{\xi}_t) \approx \alpha(d(\mathbf{x}^*, \boldsymbol{\xi}_t) - p)$ for small enough $\alpha > 0$, where $(1-\alpha)\boldsymbol{\xi}_t + \alpha\mathbf{x}^*$ is the design $\{(\mathbf{x}_i^{(t)}, (1-\alpha)w_i^{(t)}) \mid i = 1, \dots, m_t\} \bigcup \{(\mathbf{x}^*, \alpha)\}$. Thus, if we find an $\mathbf{x}^*$, such that, $d(\mathbf{x}^*, \boldsymbol{\xi}_t) > p + \epsilon$, then there exists an $\alpha_0 \in (0, 1)$, such that, $f((1-\alpha_0)\boldsymbol{\xi}_t + \alpha_0\mathbf{x}^*) - f(\boldsymbol{\xi}_t) > \alpha_0(d(\mathbf{x}^*, \boldsymbol{\xi}_t) - p)/2 > \alpha_0\epsilon/2$. For small enough merging threshold δ (see Steps 0° and 2°), we can still guarantee that $f(\boldsymbol{\xi}_{t+1}) - f(\boldsymbol{\xi}_t) > \alpha_0\epsilon/4$ after Step 2°. Under regularity conditions, $\mathcal{X}$ is compact, and $f(\boldsymbol{\xi})$ is continuous and bounded. Our algorithm is guaranteed to stop in finite steps. Actually, due to the lift-one step (Step 3°), $f(\boldsymbol{\xi}_t)$ is improved fast, especially in the first few steps. For all the examples explored in this paper, our algorithm works efficiently. □

3. D-optimal Designs for MLMs

In this section, we consider experiments with categorical responses. Following Bu et al. (2020), given $n_i > 0$ experimental units assigned to a design setting $\mathbf{x}_i \in \mathcal{X}$, the summarized responses $\mathbf{Y}_i = (Y_{i1}, \dots, Y_{iJ})^T$ follow Multinomial$(n_i; \pi_{i1}, \dots, \pi_{iJ})$ with categorical probabilities $\pi_{i1}, \dots, \pi_{iJ}$, where $J \ge 2$ is the number of categories, and Y_{ij} is the number

of experimental units with responses in the jth category. A general MLM is given by (Glonek and McCullagh, 1995; Zocchi and Atkinson, 1999; Bu et al., 2020)

$$\mathbf{C}^T \log(\mathbf{L}\boldsymbol{\pi}_i) = \boldsymbol{\eta}_i = \mathbf{X}_i\boldsymbol{\theta}, \qquad i = 1, \cdots, m \tag{3.1}$$

where $\boldsymbol{\pi}_i = (\pi_{i1}, \ldots, \pi_{iJ})^T$ satisfying $\sum_{j=1}^{J} \pi_{ij} = 1$, $\boldsymbol{\eta}_i = (\eta_{i1}, \ldots, \eta_{iJ})^T$, the matrix $\mathbf{C}^T$ has dimension $J \times (2J-1)$, $\mathbf{X}_i$ is the model matrix with dimension $J \times p$, $\boldsymbol{\theta} = (\boldsymbol{\beta}_1, \boldsymbol{\beta}_2, \cdots, \boldsymbol{\beta}_{J-1}, \boldsymbol{\zeta})^T \in \mathbb{R}^p$ are the model parameters, and $\mathbf{L}$ is a constant matrix with dimension $(2J-1) \times J$ taking different forms across four logit models, baseline-category, cumulative, adjacent-categories, and continuation-ratio (please see details in Bu et al. (2020)).

3.1 Fisher information $\mathbf{F_x}$ and sensitivity function $d(\mathbf{x}, \boldsymbol{\xi})$

The $p \times p$ matrix $\mathbf{F_x}$, known as the Fisher information at $\mathbf{x} \in \mathcal{X}$, plays a key role in the ForLion algorithm. We provide its formula in detail in Theorem 2.

Theorem 2. *For MLM* (3.1)*, the Fisher information* $\mathbf{F_x}$ *at* $\mathbf{x} \in \mathcal{X}$ *(or* $\mathcal{X}_{\boldsymbol{\theta}}$ *for cumulative logit models) is*

$$\begin{pmatrix} u_{11}^{\mathbf{x}}\mathbf{h}_1^{\mathbf{x}}(\mathbf{h}_1^{\mathbf{x}})^T & u_{12}^{\mathbf{x}}\mathbf{h}_1^{\mathbf{x}}(\mathbf{h}_2^{\mathbf{x}})^T & \cdots & u_{1,J-1}^{\mathbf{x}}\mathbf{h}_1^{\mathbf{x}}(\mathbf{h}_{J-1}^{\mathbf{x}})^T & \sum_{j=1}^{J-1} u_{1j}^{\mathbf{x}}\mathbf{h}_1^{\mathbf{x}}(\mathbf{h}_c^{\mathbf{x}})^T \\ u_{21}^{\mathbf{x}}\mathbf{h}_2^{\mathbf{x}}(\mathbf{h}_1^{\mathbf{x}})^T & u_{22}^{\mathbf{x}}\mathbf{h}_2^{\mathbf{x}}(\mathbf{h}_2^{\mathbf{x}})^T & \cdots & u_{2,J-1}^{\mathbf{x}}\mathbf{h}_2^{\mathbf{x}}(\mathbf{h}_{J-1}^{\mathbf{x}})^T & \sum_{j=1}^{J-1} u_{2j}^{\mathbf{x}}\mathbf{h}_2^{\mathbf{x}}(\mathbf{h}_c^{\mathbf{x}})^T \\ \vdots & \vdots & \ddots & \vdots & \vdots \\ u_{J-1,1}^{\mathbf{x}}\mathbf{h}_{J-1}^{\mathbf{x}}(\mathbf{h}_1^{\mathbf{x}})^T & u_{J-1,2}^{\mathbf{x}}\mathbf{h}_{J-1}^{\mathbf{x}}(\mathbf{h}_2^{\mathbf{x}})^T & \cdots & u_{J-1,J-1}^{\mathbf{x}}\mathbf{h}_{J-1}^{\mathbf{x}}(\mathbf{h}_{J-1}^{\mathbf{x}})^T & \sum_{j=1}^{J-1} u_{J-1,j}^{\mathbf{x}}\mathbf{h}_{J-1}^{\mathbf{x}}(\mathbf{h}_c^{\mathbf{x}})^T \\ \sum_{j=1}^{J-1} u_{j1}^{\mathbf{x}} \cdot \mathbf{h}_c^{\mathbf{x}}(\mathbf{h}_1^{\mathbf{x}})^T & \sum_{j=1}^{J-1} u_{j2}^{\mathbf{x}} \cdot \mathbf{h}_c^{\mathbf{x}}(\mathbf{h}_2^{\mathbf{x}})^T & \cdots & \sum_{j=1}^{J-1} u_{j,J-1}^{\mathbf{x}} \cdot \mathbf{h}_c^{\mathbf{x}}(\mathbf{h}_{J-1}^{\mathbf{x}})^T & \sum_{i=1}^{J-1}\sum_{j=1}^{J-1} u_{ij}^{\mathbf{x}} \cdot \mathbf{h}_c^{\mathbf{x}}(\mathbf{h}_c^{\mathbf{x}})^T \end{pmatrix}$$

where $\mathbf{h}_j^{\mathbf{x}} = \mathbf{h}_j(\mathbf{x})$ *and* $\mathbf{h}_c^{\mathbf{x}} = \mathbf{h}_c(\mathbf{x})$ *are predictors at* $\mathbf{x}$*, and* $u_{st}^{\mathbf{x}}$*'s are known functions of* $\mathbf{x}$ *and* $\boldsymbol{\theta}$ *(more details can be found in Section S.2 in the Supplementary Material).*

In response to Remark 1, we provide below a surprising example that the Fisher information $\mathbf{F_x}$ at a single point $\mathbf{x}$ is positive definite for almost all $\mathbf{x} \in \mathcal{X}$.

Example 1. Positive Definite $\mathbf{F_x}$ We consider a special MLM (3.1) with non-proportional odds (npo) (please see Section S.8 in the Supplementary Materials of Bu et al. (2020) for more details). Suppose $d = 1$ and a feasible design point $\mathbf{x} = x \in [a, b] = \mathcal{X}$, $J \geq 3$, $\mathbf{h}_1(\mathbf{x}) = \cdots = \mathbf{h}_{J-1}(\mathbf{x}) \equiv x$. The model matrix at $\mathbf{x} = x$ is

$$\mathbf{X}_x = \begin{pmatrix} x & 0 & \cdots & 0 \\ 0 & x & \cdots & 0 \\ \vdots & \vdots & \ddots & \vdots \\ 0 & 0 & \cdots & x \\ 0 & 0 & \cdots & 0 \end{pmatrix}_{J \times (J-1)}$$

with $p = J - 1$. Let $\boldsymbol{\theta} = (\beta_1, \ldots, \beta_{J-1})^T \in \mathbb{R}^{J-1}$ be the model parameters. Then $\mathbf{U}_x = (u_{st}^x)_{s,t=1,\ldots,J}$ can be calculated from Theorem A.2 in Bu et al. (2020). Note that $u_{sJ}^x = u_{Js}^x = 0$ for $s = 1, \ldots, J-1$ and $u_{JJ}^x = 1$. The Fisher information matrix at $\mathbf{x} = x$ is $\mathbf{F}_x = \mathbf{X}_x^T \mathbf{U}_x \mathbf{X}_x = x^2 \mathbf{V}_x$, where $\mathbf{V}_x = (u_{st}^x)_{s,t=1,\ldots,J-1}$. Then $|\mathbf{F}_x| = x^{2(J-1)}|\mathbf{V}_x|$. According to Equation (S.1) and Lemma S.9 in the supplementary material of Bu et al. (2020),

$$|\mathbf{V}_x| = \begin{cases} \prod_{j=1}^{J} \pi_j^x & \text{for baseline-category, adjacent-categories,} \\ & \text{and continuation-ratio logit models} \\ \dfrac{\left[\prod_{j=1}^{J-1} \gamma_j^x (1-\gamma_j^x)\right]^2}{\prod_{j=1}^{J} \pi_j^x} & \text{for cumulative logit models} \end{cases}$$

which is always positive, where $\gamma_j^x = \sum_{l=1}^{j} \pi_l^x \in (0, 1)$, $j = 1, \ldots, J-1$. In other words, $\mathrm{rank}(\mathbf{F}_x) = p$ in this case, as long as $x \neq 0$. □

There also exists an example of a special MLM such that $\mathbf{F_x} = \mathbf{F_{x'}}$ but $\mathbf{x} \neq \mathbf{x'}$ (see Section S.3 in the Supplementary Material).

To search for the new design point $\mathbf{x}^*$ in Step 5° of Algorithm 1, we utilize the R function `optim` with option "L-BFGS-B", which uses a limited-memory modification of the quasi-Newton method (Byrd et al., 1995) allowing box constraints. It works fairly well in finding solutions even at the boundaries of the box constraints. We give explicit formulae for computing $d(\mathbf{x}, \boldsymbol{\xi})$ below and provide the first-order derivative of the sensitivity function for MLM (3.1) in the Supplementary Material, Section S.4.

Theorem 3. *Consider MLM (3.1) with a compact $\mathcal{X}$. A design $\boldsymbol{\xi} = \{(\mathbf{x}_i, w_i), i = 1, \ldots, m\}$ with $f(\boldsymbol{\xi}) > 0$ is D-optimal if and only if $\max_{\mathbf{x} \in \mathcal{X}} d(\mathbf{x}, \boldsymbol{\xi}) \leq p$, where*

$$
\begin{aligned}
d(\mathbf{x}, \boldsymbol{\xi}) &= \sum_{j=1}^{J-1} u_{jj}^{\mathbf{x}} (\mathbf{h}_j^{\mathbf{x}})^T \mathbf{C}_{jj} \mathbf{h}_j^{\mathbf{x}} + \sum_{i=1}^{J-1} \sum_{j=1}^{J-1} u_{ij}^{\mathbf{x}} \cdot (\mathbf{h}_c^{\mathbf{x}})^T \mathbf{C}_{JJ} \mathbf{h}_c^{\mathbf{x}} \\
&\quad + 2 \sum_{i=1}^{J-2} \sum_{j=i+1}^{J-1} u_{ij}^{\mathbf{x}} (\mathbf{h}_j^{\mathbf{x}})^T \mathbf{C}_{ij} \mathbf{h}_i^{\mathbf{x}} + 2 \sum_{i=1}^{J-1} \sum_{j=1}^{J-1} u_{ij}^{\mathbf{x}} (\mathbf{h}_c^{\mathbf{x}})^T \mathbf{C}_{iJ} \mathbf{h}_i^{\mathbf{x}} \quad (3.2)
\end{aligned}
$$

$\mathbf{C}_{ij} \in \mathbb{R}^{p_i \times p_j}$ is a submatrix of the $p \times p$ matrix

$$
\mathbf{F}(\boldsymbol{\xi})^{-1} = \begin{bmatrix} \mathbf{C}_{11} & \cdots & \mathbf{C}_{1J} \\ \vdots & \ddots & \vdots \\ \mathbf{C}_{J1} & \cdots & \mathbf{C}_{JJ} \end{bmatrix}
$$

$i, j = 1, \ldots, J$, $p = \sum_{j=1}^{J} p_j$, and $p_J = p_c$. □

3.2 Example: Emergence of house flies

In this section, we revisit the motivating example at the beginning of Section 1. The original design (Itepan, 1995) assigned $n_i = 500$ pupae to each of $m = 7$ doses, $x_i = 80, 100, 120, 140, 160, 180, 200$, respectively, which corresponds to the uniform design $\boldsymbol{\xi}_u$ in Table 1. Under a continuation-ratio npo model adopted by Zocchi and Atkinson (1999)

$$
\log\left(\frac{\pi_{i1}}{\pi_{i2} + \pi_{i3}}\right) = \beta_{11} + \beta_{12} x_i + \beta_{13} x_i^2, \quad \log\left(\frac{\pi_{i2}}{\pi_{i3}}\right) = \beta_{21} + \beta_{22} x_i
$$

with fitted parameters $\boldsymbol{\theta} = (\beta_{11}, \beta_{12}, \beta_{13}, \beta_{21}, \beta_{22})^T = (-1.935, -0.02642, 0.0003174, -9.159, 0.06386)^T$, Bu et al. (2020) obtained D-optimal designs under different grid sizes by their lift-one algorithm proposed for discrete factors. With grid size 20, their design $\boldsymbol{\xi}_{20}$ contains four design points. For finer grids on $[80, 200]$, both their grid-5 design $\boldsymbol{\xi}_5$ and grid-1 design $\boldsymbol{\xi}_1$ contain five design points (see Table 1). By incorporating the Fedorov-Wynn and lift-one algorithms and continuously searching the extended region $[0, 200]$, Ai et al. (2023) obtained a four-points design $\boldsymbol{\xi}_a$ (see Example S1 in their Supplementary Material).

For $x \in \mathcal{X} = [80, 200]$ as in Bu et al. (2020), our ForLion algorithm reports $\boldsymbol{\xi}_*$ with only three design points (see Table 1, as well as the Supplementary Material, Section S.5 for details). Compared with $\boldsymbol{\xi}_*$, the relative efficiencies of the $\boldsymbol{\xi}_u$, $\boldsymbol{\xi}_{20}$, $\boldsymbol{\xi}_5$, and $\boldsymbol{\xi}_1$, defined by $[f(\cdot)/f(\boldsymbol{\xi}_*)]^{1/5}$, are 82.79%, 99.68%, 99.91%, and 99.997%, respectively. For $x \in [0, 200]$ as in Ai et al. (2023), our algorithm yields $\boldsymbol{\xi}'_*$ with only three points (see Table 1) and the relative efficiency of Ai et al. (2023)'s $\boldsymbol{\xi}_a$ with respect to $\boldsymbol{\xi}'_*$ is 99.81%. Note that both $\boldsymbol{\xi}_*$ and $\boldsymbol{\xi}'_*$ from our algorithm contain only three experimental settings, which achieves the minimum m justified by Bu et al. (2020). Given that the cost of using the radiation device is expensive and each run of the experiment takes at least hours, our designs can save 40% or 25% cost and time compared with Bu et al. (2020)'s and Ai et al. (2023)'s, respectively.

Table 1: Designs for the emergence of house files experiment

Design	$\boldsymbol{\xi}_u$	$\boldsymbol{\xi}_{20}$	$\boldsymbol{\xi}_5$	$\boldsymbol{\xi}_1$	$\boldsymbol{\xi}_*$	$\boldsymbol{\xi}_a$	$\boldsymbol{\xi}'_*$
						(0, 0.203)	(0.00, 0.2027)
	(80,0.1429)	(80, 0.3116)	(80, 0.3163)	(80, 0.3163)	(80.00, 0.3163)		
	(100,0.1429)					(101.1, 0.397)	(103.56, 0.3981)
	(120,0.1429)	(120, 0.2917)	(120, 0.1429)	(122, 0.0786)	(122.78, 0.3422)		
	(140,0.1429)	(140, 0.1071)	(125, 0.2003)	(123, 0.2636)		(147.8, 0.307)	(149.26, 0.3992)
	(160,0.1429)	(160, 0.2896)	(155, 0.1683)	(157, 0.2206)	(157.37, 0.3415)	(149.3, 0.093)	
	(180,0.1429)		(160, 0.1723)	(158, 0.1209)			
	(200,0.1429)						
Rela.Effi.	82.79%	99.68%	99.91%	99.997%	100%	99.81%	100%

To further check if the improvements by our designs are due to randomness, we conduct a simulation study by generating 100 bootstrapped replicates from the original data. For each bootstrapped data, we obtain the fitted parameters, treat them as the true values, and obtain D-optimal designs by Ai et al. (2023)'s, Bu et al. (2020)'s grid-1, and our ForLion algorithm with $\delta = 0.1$ and $\epsilon = 10^{-10}$, respectively. As Figure 1 shows, our ForLion algorithm achieves the most efficient designs with the least number of design points. Actually, the median number of design points is 5 for Ai's, 4 for Bu's, and 3 for ForLion's. Compared with ForLion's, the mean relative efficiency is 99.82% for Ai's and 99.99% for Bu's. As for computational time, the median time cost on a Windows 11 desktop with 32GB RAM and AMD Ryzen 7 5700G processor is 3.59s for Ai's, 161.81s for Bu's, and 44.88s for ForLion's.
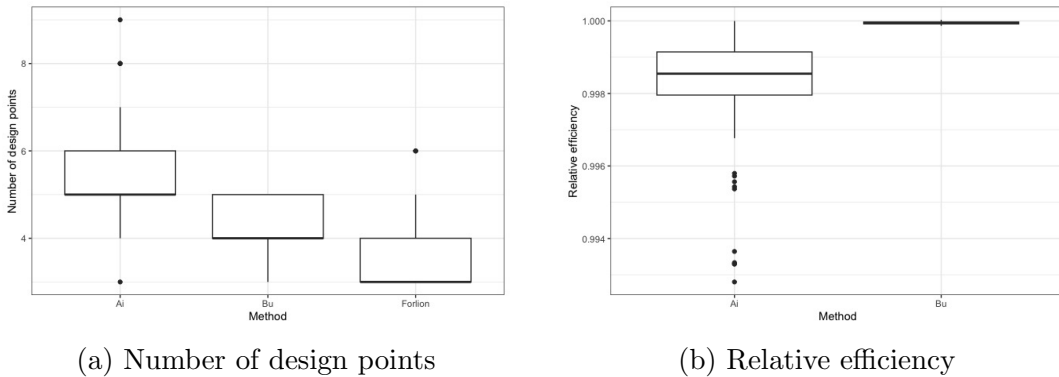

(a) Number of design points

(b) Relative efficiency

Figure 1: Boxplots of 100 bootstrapped data for Ai's, Bu's, and ForLion's designs

4. D-optimal Designs for GLMs

In this section, we consider experiments with a univariate response Y which follows a distribution $f(y; \theta) = \exp\{yb(\theta) + c(\theta) + d(y)\}$ in the exponential family with a single parameter θ. Examples include binary response $Y \sim \text{Bernoulli}(\theta)$, count response $Y \sim \text{Poisson}(\theta)$, positive response $Y \sim \text{Gamma}(k, \theta)$ with known $k > 0$, and continuous response $Y \sim N(\theta, \sigma^2)$ with known $\sigma^2 > 0$ (McCullagh and Nelder, 1989). Suppose independent responses $Y_1, \ldots, Y_n$ are collected with corresponding factor level combinations $\mathbf{x}_1, \ldots, \mathbf{x}_n \in \mathcal{X} \subset \mathbb{R}^d$, where $\mathbf{x}_i = (x_{i1}, \ldots, x_{id})^T$. Under a generalized linear model (GLM), there exist a link function g, parameters of interest $\boldsymbol{\beta} = (\beta_1, \beta_2, \ldots, \beta_p)^T$, and the corresponding vector of p known and deterministic predictor functions $\mathbf{h} = (h_1, \ldots, h_p)^T$, such that

$$E(Y_i) = \mu_i \text{ and } \eta_i = g(\mu_i) = \mathbf{X}_i^T \boldsymbol{\beta} \tag{4.3}$$

where $\mathbf{X}_i = \mathbf{h}(\mathbf{x}_i) = (h_1(\mathbf{x}_i), \ldots, h_p(\mathbf{x}_i))^T$, $i = 1, \ldots, n$. For many applications, $h_1(\mathbf{x}_i) \equiv 1$ represents the intercept of the model.

4.1 ForLion algorithm specialized for GLM

Due to the specific form of GLM's Fisher information (see Section S.7 and (S7.9) in the Supplementary Material), the lift-one algorithm can be extremely efficient by utilizing analytic solutions for each iteration (Yang and Mandal, 2015). In this section, we specialize the ForLion algorithm for GLM with explicit formulae in Steps 3°, 5°, and 6°.

For GLM (4.3), our goal is to find a design $\boldsymbol{\xi} = \{(\mathbf{x}_i, w_i), i = 1, \ldots, m\}$ maximizing $f(\boldsymbol{\xi}) = |\mathbf{X}_{\boldsymbol{\xi}}^T \mathbf{W}_{\boldsymbol{\xi}} \mathbf{X}_{\boldsymbol{\xi}}|$, where $\mathbf{X}_{\boldsymbol{\xi}} = (\mathbf{h}(\mathbf{x}_1), \ldots, \mathbf{h}(\mathbf{x}_m))^T \in \mathbb{R}^{m \times p}$ with known predictor functions $h_1, \ldots, h_p$, and $\mathbf{W}_{\boldsymbol{\xi}} = \text{diag}\{w_1 \nu(\boldsymbol{\beta}^T \mathbf{h}(\mathbf{x}_1)), \ldots, w_m \nu(\boldsymbol{\beta}^T \mathbf{h}(\mathbf{x}_m))\}$ with known parameters $\boldsymbol{\beta} = (\beta_1, \ldots, \beta_p)^T$ and a positive differentiable function ν. The sensitivity function $d(\mathbf{x}, \boldsymbol{\xi}) = \text{tr}(\mathbf{F}(\boldsymbol{\xi})^{-1} \mathbf{F}_{\mathbf{x}})$ in Step 5° of Algorithm 1 can be written as $\nu(\boldsymbol{\beta}^T \mathbf{h}(\mathbf{x})) \cdot \mathbf{h}(\mathbf{x})^T (\mathbf{X}_{\boldsymbol{\xi}}^T \mathbf{W}_{\boldsymbol{\xi}} \mathbf{X}_{\boldsymbol{\xi}})^{-1} \mathbf{h}(\mathbf{x})$. As a direct conclusion of the general equivalence theorem (see Theorem 2.2 in Fedorov and Leonov (2014)), we have the following theorem for GLMs.

Theorem 4. *Consider GLM* (4.3) *with a compact design region* $\mathcal{X}$. *A design* $\boldsymbol{\xi} = \{(\mathbf{x}_i, w_i), i = 1, \ldots, m\}$ *with* $f(\boldsymbol{\xi}) = |\mathbf{X}_{\boldsymbol{\xi}}^T \mathbf{W}_{\boldsymbol{\xi}} \mathbf{X}_{\boldsymbol{\xi}}| > 0$ *is D-optimal if and only if*

$$\max_{\mathbf{x} \in \mathcal{X}} \nu(\boldsymbol{\beta}^T \mathbf{h}(\mathbf{x})) \cdot \mathbf{h}(\mathbf{x})^T (\mathbf{X}_{\boldsymbol{\xi}}^T \mathbf{W}_{\boldsymbol{\xi}} \mathbf{X}_{\boldsymbol{\xi}})^{-1} \mathbf{h}(\mathbf{x}) \leq p \tag{4.4}$$

Given the design $\boldsymbol{\xi}_t = \{(\mathbf{x}_i^{(t)}, w_i^{(t)}), i = 1, \ldots, m_t\}$ at the tth iteration, suppose in Step 5° we find the design point $\mathbf{x}^* \in \mathcal{X}$ maximizing $d(\mathbf{x}, \boldsymbol{\xi}_t) = \nu(\boldsymbol{\beta}^T \mathbf{h}(\mathbf{x})) \cdot \mathbf{h}(\mathbf{x})^T (\mathbf{X}_{\boldsymbol{\xi}_t}^T \mathbf{W}_{\boldsymbol{\xi}_t} \mathbf{X}_{\boldsymbol{\xi}_t})^{-1} \mathbf{h}(\mathbf{x})$ according to Theorem 4. Recall that $d(\mathbf{x}^*, \boldsymbol{\xi}_t) \leq p$ in this step implies the optimality of $\boldsymbol{\xi}_t$ and the end of the iterations. If $d(\mathbf{x}^*, \boldsymbol{\xi}_t) > p$, $\mathbf{x}^*$ will be added to form the updated design $\boldsymbol{\xi}_{t+1}$. For GLMs, instead of letting $\boldsymbol{\xi}_{t+1} = \boldsymbol{\xi}_t \bigcup \{(\mathbf{x}^*, 0)\}$, we recommend $(1 - \alpha_t)\boldsymbol{\xi}_t \bigcup \{(\mathbf{x}^*, \alpha_t)\}$ with α_t determined by Theorem 5, where $(1 - \alpha_t)\boldsymbol{\xi}_t$ represents $\{(\mathbf{x}_i^{(t)}, (1 - \alpha_t)w_i^{(t)}), i = 1, \ldots, m_t\}$.

Theorem 5. *Given $\boldsymbol{\xi}_t = \{(\mathbf{x}_i^{(t)}, w_i^{(t)}), i = 1, \ldots, m_t\}$ and $\mathbf{x}^* \in \mathcal{X}$, if we consider $\boldsymbol{\xi}_{t+1}$ in the form of $(1 - \alpha)\boldsymbol{\xi}_t \bigcup \{(\mathbf{x}^*, \alpha)\}$ with $\alpha \in [0, 1]$, then*

$$
\alpha_t = \begin{cases} \frac{2^p \cdot d_t - (p+1)b_t}{p(2^p \cdot d_t - 2b_t)} & \text{if } 2^p \cdot d_t > (p+1)b_t \\ 0 & \text{otherwise} \end{cases}
$$

maximizes $f(\boldsymbol{\xi}_{t+1})$ with $d_t = f(\{(\mathbf{x}_1^{(t)}, w_1^{(t)}/2), \ldots, (\mathbf{x}_{m_t}^{(t)}, w_{m_t}^{(t)}/2), (\mathbf{x}^*, 1/2)\})$ and $b_t = f(\boldsymbol{\xi}_t)$.

Based on α_t in Theorem 5, which is obtained essentially via one iteration of the lift-one algorithm (Yang et al., 2016; Yang and Mandal, 2015) with $\mathbf{x}^*$ added, we update Step 6° of Algorithm 1 with Step 6′ for GLMs, which speeds up the ForLion algorithm significantly.

6′ If $d(\mathbf{x}^*, \boldsymbol{\xi}_t) \leq p$, go to Step 7°. Otherwise, we let $\boldsymbol{\xi}_{t+1} = (1 - \alpha_t)\boldsymbol{\xi}_t \bigcup \{(\mathbf{x}^*, \alpha_t)\}$, replace t by $t + 1$, and go back to Step 2°, where α_t is given by Theorem 5.

The advantages of the lift-one algorithm over commonly used numerical algorithms include simplified computation and exact zero weight for negligible design points. For GLMs, Step 3° of Algorithm 1 should be specialized with analytic iterations as in Yang and Mandal (2015). We provide the explicit formula for the sensitivity function's first-order derivative in Section S.8 of the Supplementary Material for Step 5°.

By utilizing the analytical solutions for GLM in Steps 3°, 5° and 6′, the computation is much faster than the general procedure of the ForLion algorithm (see Example 2).

4.2 Minimally supported design and initial design

A minimally supported design $\boldsymbol{\xi} = \{(\mathbf{x}_i, w_i), i = 1, \ldots, m\}$ achieves the smallest possible m such that $f(\boldsymbol{\xi}) > 0$, or equivalently, the Fisher information matrix is of full rank. Due to the existence of Example 1, m could be as small as 1 for an MLM. Nevertheless, m must be p or above for GLMs due to the following theorem.

Theorem 6. *Consider a design $\boldsymbol{\xi} = \{(\mathbf{x}_i, w_i), i = 1, \ldots, m\}$ with m support points, that is, $w_i > 0$, $i = 1, \ldots, m$, for model (4.3). Then $f(\boldsymbol{\xi}) > 0$ only if $\mathbf{X}_{\boldsymbol{\xi}}$ is of full column rank p, that is, $\mathrm{rank}(\mathbf{X}_{\boldsymbol{\xi}}) = p$. Therefore, a minimally supported design contains at least p support points. Furthermore, if $\nu(\boldsymbol{\beta}^T \mathbf{h}(\mathbf{x})) > 0$ for all $\mathbf{x}$ in the design region $\mathcal{X}$, then $f(\boldsymbol{\xi}) > 0$ if and only if $\mathrm{rank}(\mathbf{X}_{\boldsymbol{\xi}}) = p$.*

Theorem 7 shows a minimally supported design for a GLM must be a uniform design.

Theorem 7. *Consider a minimally supported design $\boldsymbol{\xi} = \{(\mathbf{x}_i, w_i), i = 1, \ldots, p\}$ for model (4.3) that satisfies $f(\boldsymbol{\xi}) > 0$. It is D-optimal only if $w_i = p^{-1}$, $i = 1, \ldots, p$. That is, it is a uniform allocation on the support points.*

Based on Theorem 7, we recommend a minimally supported design as the initial design for ForLion algorithm under GLMs. The advantage is that once p design points $\mathbf{x}_1, \ldots, \mathbf{x}_p$ are chosen from $\mathcal{X}$, such that the model matrix $\mathbf{X}_{\boldsymbol{\xi}} = (\mathbf{h}(\mathbf{x}_1), \ldots, \mathbf{h}(\mathbf{x}_p))^T$ is

of full rank p, then the design $\boldsymbol{\xi} = \{(\mathbf{x}_i, 1/p), i = 1, \ldots, p\}$ is D-optimal given those p design points.

Recall that a typical design space can take the form of $\mathcal{X} = \prod_{j=1}^{d} I_j$, where I_j is either a finite set of distinct numerical levels or an interval $[a_j, b_j]$, and $a_j = \min I_j$ and $b_j = \max I_j$ even if I_j is a finite set. As one option in Step $1°$ of Algorithm 1, we suggest to choose p initial design points from $\prod_{j=1}^{d} \{a_j, b_j\}$. For typical applications, we may assume that there exist p distinct points in $\prod_{j=1}^{d} \{a_j, b_j\}$ such that the corresponding model matrix $\mathbf{X}_{\boldsymbol{\xi}}$ is of full rank, or equivalently, the $2^d \times p$ matrix consisting of rows $\mathbf{h}(\mathbf{x})^T, \mathbf{x} \in \prod_{j=1}^{d} \{a_j, b_j\}$ is of full rank p. Herein, we specialize Step $1°$ of Algorithm 1 for GLMs as follows:

$1'$ Construct an initial design $\boldsymbol{\xi}_0 = \{(\mathbf{x}_i^{(0)}, p^{-1}), i = 1, \ldots, p\}$ such that $\mathbf{x}_1^{(0)}, \ldots, \mathbf{x}_p^{(0)} \in \prod_{j=1}^{d} \{a_j, b_j\}$ and $\mathbf{X}_{\boldsymbol{\xi}_0} = (\mathbf{h}(\mathbf{x}_1^{(0)}), \ldots, \mathbf{h}(\mathbf{x}_p^{(0)}))^T$ is of full rank p.

4.3 Examples under GLMs

In this section, we use two examples to show the performance of our ForLion algorithm under GLMs, both with continuous factors involved only as main effects, which have simplified notations (see Section S.9 in the Supplementary Material).

Example 2. In Example 4.7 of Stufken and Yang (2012), they considered a logistic model with three continuous factors $\text{logit}(\mu_i) = \beta_0 + \beta_1 x_{i1} + \beta_2 x_{i2} + \beta_3 x_{i3}$ with $x_{i1} \in [-2, 2]$, $x_{i2} \in [-1, 1]$, and $x_{i3} \in (-\infty, \infty)$. Assuming $(\beta_0, \beta_1, \beta_2, \beta_3) = (1, -0.5, 0.5, 1)$, they obtained an 8 points D-optimal design $\boldsymbol{\xi}_o$ theoretically. Using a MacOS-based laptop with CPU 2 GHz Quad-Core and memory 16GB 3733 MHz, our ForLion algorithm specialized for GLMs takes 17 seconds and our general ForLion algorithm takes 124 seconds to get the same design $\boldsymbol{\xi}_*$ (see Table 2). The relative efficiency of $\boldsymbol{\xi}_*$ compared with $\boldsymbol{\xi}_o$ is simply 100%. Note that $\boldsymbol{\xi}_o$ was obtained from an analytic approach requiring an unbounded x_{i3}. For bounded x_{i3}, such as $x_{i3} \in [-1, 1]$, $[-2, 2]$, or $[-3, 3]$, we can still use the ForLion algorithm to obtain the corresponding D-optimal designs, whose relative efficiencies compared with $\boldsymbol{\xi}_o$ or $\boldsymbol{\xi}_*$ are 85.55%, 99.13%, and 100.00%, respectively. □

Table 2: Designs Obtained for Example 2

	Stufken and Yang (2012)'s $\boldsymbol{\xi}_o$				ForLion's $\boldsymbol{\xi}_*$			
i	x_{i1}	x_{i2}	x_{i3}	w_i	x_{i1}	x_{i2}	x_{i3}	w_i
1	-2	-1	-2.5436	0.125	-2	-1	-2.5433	0.125
2	-2	-1	-0.4564	0.125	-2	-1	-0.4565	0.125
3	-2	1	-3.5436	0.125	-2	1	-3.5433	0.125
4	-2	1	-1.4564	0.125	-2	1	-1.4564	0.125
5	2	-1	-0.5436	0.125	2	-1	-0.5435	0.125
6	2	-1	1.5436	0.125	2	-1	1.5434	0.125
7	2	1	-1.5436	0.125	2	1	-1.5445	0.125
8	2	1	0.5436	0.125	2	1	0.5433	0.125

Example 3. Lukemire et al. (2019) reconsidered the electrostatic discharge (ESD) experiment described by Whitman et al. (2006) with a binary response and five mixed factors. The first four factors `LotA`, `LotB`, `ESD`, `Pulse` take values in $\{-1, 1\}$, and the

fifth factor `Voltage` $\in [25, 45]$ is continuous. Using their d-QPSO algorithm, Lukemire et al. (2019) obtained a 13-points design $\boldsymbol{\xi}_o$ for the model $\text{logit}(\mu) = \beta_0 + \beta_1\texttt{LotA} + \beta_2\texttt{LotB} + \beta_3\texttt{ESD} + \beta_4\texttt{Pulse} + \beta_5\texttt{Voltage} + \beta_{34}(\texttt{ESD} \times \texttt{Pulse})$ with assumed parameter values $\boldsymbol{\beta} = (-7.5, 1.50, -0.2, -0.15, 0.25, 0.35, 0.4)^T$. It takes 88 seconds using the same laptop as in Example 2 for our (GLM) ForLion algorithm to find a slightly better design $\boldsymbol{\xi}_*$ consisting of 14 points (see Table S.2 in the Supplementary Material) with relative efficiency $[f(\boldsymbol{\xi}_*)/f(\boldsymbol{\xi}_o)]^{1/7} = 100.08\%$.

To make a thorough comparison, we randomly generate 100 sets of parameters $\boldsymbol{\beta}$ from independent uniform distributions: $U(1.0, 2.0)$ for `LotA`, $U(-0.3, -0.1)$ for `LotB`, $U(-0.3, 0.0)$ for `ESD`, $U(0.1, 0.4)$ for `Pulse`, $U(0.25, 0.45)$ for `Voltage`, $U(0.35, 0.45)$ for `ESD`×`Pulse`, and $U(-8.0, -7.0)$ for Intercept. For each simulated $\boldsymbol{\beta}$, we treat it as the true parameter values and obtain D-optimal designs using d-QPSO, ForLion, and Fedorov-Wynn-liftone (that is, the ForLion algorithm without the merging step, similar in spirit to Ai et al. (2023)'s) algorithms. For the ForLion algorithm, we use $\delta = 0.03$ and $\epsilon = 10^{-8}$ (see Section S.10 in the Supplementary Material for more discussion on choosing δ). For the d-QPSO algorithm, following Lukemire et al. (2019), we use 5 swarms with 30 particles each and the algorithm searches design with up to 18 support points and the maximum number of iterations $4,000$. Figure 2 shows the numbers of design points of the three algorithms and the relative efficiencies. The median number of design points is 13 for d-QPSO's, 39 for Fedorov-Wynn-liftone's, and 13 for Forlion's. The mean relative efficiencies compared with our ForLion D-optimal designs, defined as $[f(\cdot)/f(\boldsymbol{\xi}_{\text{ForLion}})]^{1/7}$, is 86.95% for d-QPSO's and 100% for Fedorov-Wynn-liftone's. The median running time on the same desktop in Section 3.2 is 10.94s for d-QPSO's, 129.74s for Fedorov-Wynn-liftone's, and 71.21s for ForLion's. $\qquad\square$

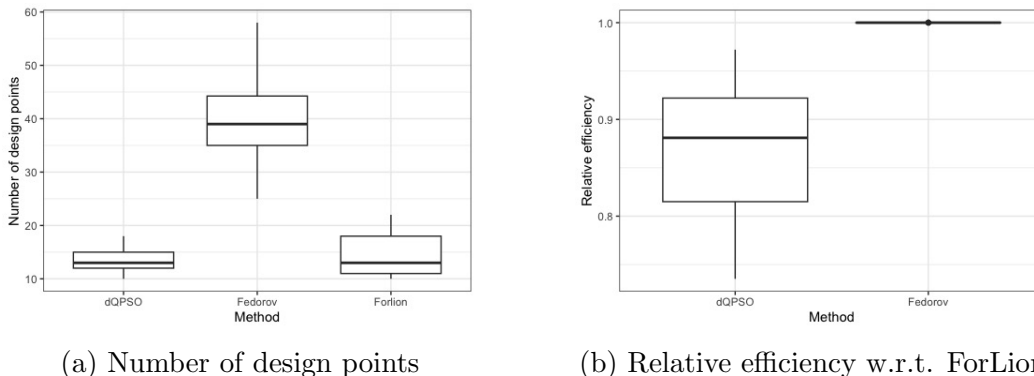(a) Number of design points   (b) Relative efficiency w.r.t. ForLion

Figure 2: Boxplots of 100 simulations for d-QPSO, Fedorov-Wynn-liftone, and ForLion algorithms for the electrostatic discharge experiment (Example 3)

5. Conclusion

In this paper, we develop the ForLion algorithm to find D-optimal designs under fairly general parametric models with mixed factors. Compared with Bu et al. (2020)'s and Ai

et al. (2023)'s algorithm, our ForLion algorithm can reduce the number of distinct experimental settings by 25% above on average while keeping the highest possible efficiency (see Section 3.2). Compared with PSO-type algorithms, the ForLion algorithm can improve the relative efficiency by 17.5% above on average while achieving a low number of distinct experimental settings (see Example 3).

SUPPLEMENTARY MATERIAL

S.1 Commonly used GLMs: A list of commonly used GLM models, corresponding link functions, ν functions, and their first-order derivatives; **S.2 Computing $u_{st}^{\mathbf{x}}$ in Fisher information $\mathbf{F_x}$:** Formulae of $u_{st}^{\mathbf{x}}$ in Fisher information; **S.3 Example that $\mathbf{F_x} = \mathbf{F_{x'}}$ with $\mathbf{x} \neq \mathbf{x'}$:** A special MLM example that $\mathbf{F_x} = \mathbf{F_{x'}}$ but $\mathbf{x} \neq \mathbf{x'}$; **S.4 First-order derivative of sensitivity function:** Formulae of $\frac{\partial d(\mathbf{x},\boldsymbol{\xi})}{\partial x_i}$ for applying quasi-Newton method; **S.5 Technical details of house flies example:** Technical details of applying the ForLion algorithm to the emergence of house flies example; **S.6 Example: Minimizing surface defects:** An example with cumulative logit po model that shows the advantages of the ForLion algorithm; **S.7 Fisher information matrix for GLMs:** Formulae for computing Fisher information matrix for GLMs; **S.8 First-order derivative of sensitivity function for GLMs:** Formulae of $\frac{\partial d(\mathbf{x},\boldsymbol{\xi})}{\partial x_i}$ for GLMs; **S.9 GLMs with main-effects continuous factors:** Details of GLMs with main-effects continuous factors; **S.10 Electrostatic discharge example supplementary:** The optimal design table for electrostatic discharge example and a simulation study on the effects of merging threshold δ; **S.11 Proofs:** Proofs for theorems in this paper.

References

Ai, M., Ye, Z., and Yu, J. (2023), "Locally D-Optimal Designs for Hierarchical Response Experiments," *Statistica Sinica*, 33, 381–399.

Atkinson, A., Donev, A., and Tobias, R. (2007), *Optimum Experimental Designs, with SAS*, Oxford University Press.

Box, G. E., and Cox, D. R. (1964), "An analysis of transformations," *Journal of the Royal Statistical Society Series B: Statistical Methodology*, 26, 211–243.

Bu, X., Majumdar, D., and Yang, J. (2020), "D-optimal Designs for Multinomial Logistic Models," *Annals of Statistics*, 48, 983–1000.

Byrd, R., Lu, P., Nocedal, J., and Zhu, C. (1995), "A limited memory algorithm for bound constrained optimization," *SIAM Journal on Scientific Computing*, 16, 1190–1208.

Christensen, R. H. B. (2015), "Analysis of ordinal data with cumulative link models—estimation with the R-package ordinal," *R-package version*, 28, 406.

Fedorov, V. (1972), *Theory of Optimal Experiments*, Academic Press.

Fedorov, V., and Leonov, S. (2014), *Optimal Design for Nonlinear Response Models*, Chapman & Hall/CRC.

Fedorov, V. V., and Hackl, P. (1997), *Model-Oriented Design of Experiments*, Springer Science & Business Media.

Glonek, G., and McCullagh, P. (1995), "Multivariate logistic models," *Journal of the Royal Statistical Society, Series B*, 57, 533–546.

Huang, Y., Tong, L., and Yang, J. (2023), "Constrained D-optimal design for paid research study," *Statistica Sinica*, to appear, available at `https://www3.stat.sinica.edu.tw/ss_newpaper/SS-2022-0414_na.pdf`.

Itepan, N. M. (1995), "Aumento do periodo de aceitabilidade de pupas de musca domestica l., 1758 (diptera: muscidae), irradiadas com raios gama, como hospedeira de parasitoides (hymenoptera: pteromalidae)," Master's thesis, Universidade de São Paulo.

Kennedy, J., and Eberhart, R. (1995), "Particle swarm optimization," in *Proceedings of ICNN'95-International Conference on Neural Networks*, IEEE, vol. 4, pp. 1942–1948.

Kiefer, J. (1974), "General equivalence theory for optimum designs (approximate theory)," *Annals of Statistics*, 2, 849–879.

Liu, C. (2004), in *Applied Bayesian modeling and causal inference from incomplete-data perspectives*, eds. Gelman, A., and Meng, X., Wiley, pp. 227–238.

Lukemire, J., Mandal, A., and Wong, W. K. (2019), "d-QPSO: A quantum-behaved particle swarm technique for finding D-optimal designs with discrete and continuous factors and a binary response," *Technometrics*, 61, 77–87.

Lukemire, J., Mandal, A.— (2022), "Optimal experimental designs for ordinal models with mixed factors for industrial and healthcare applications," *Journal of Quality Technology*, 54, 184–196.

McCullagh, P., and Nelder, J. (1989), *Generalized Linear Models*, Chapman and Hall/CRC, 2nd ed.

Nocedal, J., and Wright, S. (1999), *Numerical Optimization*, Springer.

Phadke, M. (1989), *Quality Engineering using Robust Design*, Prentice-Hall, Englewood Cliffs.

Poli, R., Kennedy, J., and Blackwell, T. (2007), "Particle swarm optimization: An overview," *Swarm Intelligence*, 1, 33–57.

Pukelsheim, F. (1993), *Optimal Design of Experiments*, John Wiley & Sons.

Seber, G. (2008), *A Matrix Handbook for Statisticians*, Wiley.

Silvey, S., Titterington, D., and Torsney, B. (1978), "An algorithm for optimal designs on a finite design space," *Communications in Statistics - Theory and Methods*, 14, 1379–1389.

Stufken, J., and Yang, M. (2012), "Optimal designs for generalized linear models," in *Design and Analysis of Experiments, Volume 3: Special Designs and Applications*, ed. Hinkelmann, K., Wiley, chap. 4, pp. 137–164.

Titterington, D. (1976), "Algorithms for computing D-optimal design on finite design spaces," in *Proc. of the 1976 Conf. on Information Science and Systems*, John Hopkins University, vol. 3, pp. 213–216.

— (1978), "Estimation of correlation coefficients by ellipsoidal trimming," *Journal of the Royal Statistical Society, Series C (Applied Statistics)*, 27, 227–234.

Venables, W. N., and Ripley, B. D. (2002), *Modern Applied Statistics with S*, Springer, 4th ed.

Whitman, C., Gilbert, T., Rahn, A., and Antonell, J. (2006), "Determining factors affecting ESD failure voltage using DOE," *Microelectronics Reliability*, 46, 1228–1237.

Wu, F.-C. (2008), "Simultaneous optimization of robust design with quantitative and ordinal data," *International Journal of Industrial Engineering: Theory, Applications and Practice*, 5, 231–238.

Yang, J., and Mandal, A. (2015), "D-optimal factorial designs under generalized linear models," *Communications in Statistics - Simulation and Computation*, 44, 2264–2277.

Yang, J., Mandal, A., and Majumdar, D. (2016), "Optimal designs for 2^k factorial experiments with binary response," *Statistica Sinica*, 26, 385–411.

Yang, J., Tong, L., and Mandal, A. (2017), "D-optimal designs with ordered categorical data," *Statistica Sinica*, 27, 1879–1902.

Yang, M., Biedermann, S., and Tang, E. (2013), "On optimal designs for nonlinear models: a general and efficient algorithm," *Journal of the American Statistical Association*, 108, 1411–1420.

Yu, Y. (2011), "D-optimal designs via a cocktail algorithm," *Statistics and Computing*, 21, 475–481.

Zocchi, S., and Atkinson, A. (1999), "Optimum experimental designs for multinomial logistic models," *Biometrics*, 55, 437–444.

ForLion: A New Algorithm for D-optimal Designs under General Parametric Statistical Models with Mixed Factors

Yifei Huang[1], Keren Li[2], Abhyuday Mandal[3], and Jie Yang[1]

[1]University of Illinois at Chicago, [2]University of Alabama at Birmingham, and [3]University of Georgia

Supplementary Material

S.1 Commonly used GLMs: A list of commonly used GLM models, corresponding link functions, ν functions, and their first-order derivatives;

S.2 Computing $u_{st}^{\mathbf{x}}$ in Fisher information $\mathbf{F_x}$: Formulae of $u_{st}^{\mathbf{x}}$ in Fisher information;

S.3 Example that $\mathbf{F_x} = \mathbf{F_{x'}}$ with $\mathbf{x} \neq \mathbf{x'}$: A special MLM example that $\mathbf{F_x} = \mathbf{F_{x'}}$ but $\mathbf{x} \neq \mathbf{x'}$;

S.4 First-order derivative of sensitivity function: Formulae of $\frac{\partial d(\mathbf{x}, \boldsymbol{\xi})}{\partial x_i}$ for applying quasi-Newton method;

S.5 Technical details of house flies example: Technical details of applying the ForLion algorithm to the emergence of house flies example;

S.6 Example: Minimizing surface defects: An example with cumulative logit po model that shows the advantages of the ForLion algorithm;

S.7 Fisher information matrix for GLMs: Formulae for computing Fisher information matrix for GLMs;

S.8 First-order derivative of sensitivity function for GLMs: Formulae of $\frac{\partial d(\mathbf{x}, \boldsymbol{\xi})}{\partial x_i}$ for GLMs;

S.9 GLMs with main-effects continuous factors: Details of GLMs with main-effects continuous factors;

S.10 Electrostatic discharge example supplementary: The optimal design table for electrostatic discharge example and a simulation study on the effects of merging threshold δ;

S.11 Proofs: Proofs for theorems in this paper.

S.1. Commonly used GLMs

In this section, we provide the formulae of the link function, $\nu(\eta)$, and $\nu'(\eta)$ for commonly used GLMs, which are needed for the ForLion algorithm (see Section 4.1, as well as Sections S.7, S.8, and S.9 in the Supplementary Material).

1. Bernoulli(μ) with logit link
   Link function: $\eta = g(\mu) = \log(\mu/(1-\mu))$;
   $\nu(\eta) = e^\eta/(1 + e^\eta)^2$;
   $\nu'(\eta) = -e^\eta(e^\eta - 1)/(1 + e^\eta)^3$.

2. Bernoulli(μ) with probit link
   Link function: $\eta = g(\mu) = \Phi^{-1}(\mu)$;
   $\nu(\eta) = \phi(\eta)^2/\{\Phi(\eta)[1 - \Phi(\eta)]\}$;

   $$\nu'(\eta) = -\frac{2\eta\phi^2(\eta)}{[1 - \Phi(\eta)]\Phi(\eta)} + \frac{\phi^3(\eta)[2\Phi(\eta) - 1]}{[1 - \Phi(\eta)]^2\Phi^2(\eta)}$$

   Note that $\phi'(\eta) = -\eta\phi(\eta)$ and $\phi''(\eta) = (\eta^2 - 1)\phi(\eta)$.

3. Bernoulli(μ) with cloglog link
   Link function: $\eta = g(\mu) = \log(-\log(1-\mu))$;
   $\nu(\eta) = e^{2\eta}/(\exp\{e^\eta\} - 1)$;

   $$\nu'(\eta) = \frac{2e^{2\eta}}{\exp\{e^\eta\} - 1} - \frac{\exp\{3\eta + e^\eta\}}{(\exp\{e^\eta\} - 1)^2}$$

4. Bernoulli(μ) with loglog link

 Link function: $\eta = g(\mu) = \log(-\log\mu)$;

 In this case, $\nu(\eta)$, $\nu'(\eta)$, are exactly the same as Bernoulli(μ) with cloglog link. An alternative (strictly increase) loglog link (Yang et al., 2017) is $\eta = g(\mu) = -\log(-\log\mu)$. Then $\nu(\eta) = \exp\{-2\eta\}/[\exp\{e^{-\eta}\} - 1]$.

5. Bernoulli(μ) with cauchit link

 Link function: $\eta = g(\mu) = \tan(\pi(\mu - 1/2))$;

 $\nu(\eta) = (1 + \eta^2)^{-2}[\pi^2/4 - \arctan^2(\eta)]^{-1}$;

$$\nu'(\eta) \;=\; \frac{16}{(1+\eta^2)^3}\left(\frac{-\eta}{\pi^2 - 4\arctan^2(\eta)} + \frac{2\arctan(\eta)}{[\pi^2 - 4\arctan^2(\eta)]^2}\right)$$

6. Bernoulli(μ) with t link (Liu, 2004)

 Link function: $\eta = g(\mu) = F_\nu^{-1}(\mu)$, where F_ν is the cumulative distribution function of t distribution with degrees of freedom $\nu > 0$;

 $(g^{-1})'(\eta) = f_\nu(\eta) = \frac{\Gamma\left(\frac{\nu+1}{2}\right)}{\sqrt{\nu\pi}\,\Gamma\left(\frac{\nu}{2}\right)}\left(1 + \frac{\eta^2}{\nu}\right)^{-\frac{\nu+1}{2}}$, where f_ν is the probability density function of t distribution with degrees of freedom $\nu > 0$. Then

$$\nu(\eta) \;=\; \frac{f_\nu^2(\eta)}{F_\nu(\eta)\left[1 - F_\nu(\eta)\right]}$$

$$\nu'(\eta) \;=\; -\frac{2\eta f_\nu^2(\eta)}{[1 - F_\nu(\eta)]F_\nu(\eta)} + \frac{f_\nu^3(\eta)[2F_\nu(\eta) - 1]}{[1 - F_\nu(\eta)]^2 F_\nu^2(\eta)}$$

7. Poisson(μ) with log link

 Link function: $\eta = g(\mu) = \log(\mu)$;

 $\nu(\eta) = \nu'(\eta) = e^\eta$.

8. Gamma(k, μ/k) with reciprocal link, $k > 0$ is known

 Link function: $\eta = g(\mu) = \mu^{-1}$, $\mu > 0$;

 $\nu(\eta) = k\eta^{-2}$;

 $\nu'(\eta) = -2k\eta^{-3}$.

9. Normal(μ, σ^2) with identify link, that is, the usual linear regression model

 Link function: $\eta = g(\mu) = \mu$;

 $\nu(\eta) \equiv \sigma^{-2}$; $\nu'(\eta) = 0$.

10. Inverse Gaussian(μ, λ) with inverse squared link, $\lambda > 0$ is known

 Link function: $\eta = g(\mu) = \mu^{-2}$;

 $\nu(\eta) = \frac{\lambda}{4}\eta^{-3/2}$;

 $\nu'(\eta) = -\frac{3}{8}\lambda\eta^{-5/2}$.

S.2.   Computing u_{st}^{x} in Fisher information $\mathbf{F_x}$

In this section, we provide more technical details for Section 3.1 and Theorem 2.

For MLM (3.1), Corollary 3.1 in Bu et al. (2020) provided an alternative form $\mathbf{F}_{\mathbf{x}_i} = \mathbf{X}_i^T \mathbf{U}_i \mathbf{X}_i$, which we will use for computing the Fisher information $\mathbf{F}_\mathbf{x}$ at an arbitrary $\mathbf{x} \in \mathcal{X}$. More specifically, first of all, the corresponding model matrix at $\mathbf{x}$ is

$$\mathbf{X}_\mathbf{x} = \begin{pmatrix} \mathbf{h}_1^T(\mathbf{x}) & \mathbf{0}^T & \cdots & \mathbf{0}^T & \mathbf{h}_c^T(\mathbf{x}) \\ \mathbf{0}^T & \mathbf{h}_2^T(\mathbf{x}) & \ddots & \vdots & \vdots \\ \vdots & \ddots & \ddots & \mathbf{0}^T & \mathbf{h}_c^T(\mathbf{x}) \\ \mathbf{0}^T & \cdots & \mathbf{0}^T & \mathbf{h}_{J-1}^T(\mathbf{x}) & \mathbf{h}_c^T(\mathbf{x}) \\ \mathbf{0}^T & \cdots & \cdots & \mathbf{0}^T & \mathbf{0}^T \end{pmatrix}_{J \times p} \tag{S2.1}$$

where $\mathbf{h}_j^T(\cdot) = (h_{j1}(\cdot), \ldots, h_{jp_j}(\cdot))$ and $\mathbf{h}_c^T(\cdot) = (h_1(\cdot), \ldots, h_{p_c}(\cdot))$ are known predictor functions. Given the model parameter $\boldsymbol{\theta} = (\boldsymbol{\beta}_1, \boldsymbol{\beta}_2, \cdots, \boldsymbol{\beta}_{J-1}, \boldsymbol{\zeta})^T \in \mathbb{R}^p$, the linear predictor $\boldsymbol{\eta}_\mathbf{x} = \mathbf{X}_\mathbf{x} \boldsymbol{\theta} = (\eta_1^\mathbf{x}, \ldots, \eta_{J-1}^\mathbf{x}, 0)^T \in \mathbb{R}^J$, where $\eta_j^\mathbf{x} = \mathbf{h}_j^T(\mathbf{x})\boldsymbol{\beta}_j + \mathbf{h}_c^T(\mathbf{x})\boldsymbol{\zeta}$, $j = 1, \ldots, J-1$.

According to Lemmas S.10, S.12 and S.13 in the Supplementary Materials of Bu et al. (2020), the categorical probabilities $\boldsymbol{\pi}_\mathbf{x} = (\pi_1^\mathbf{x}, \ldots, \pi_J^\mathbf{x})^T \in \mathbb{R}^J$ at $\mathbf{x}$ for baseline-category, adjacent-categories and continuation-ratio logit models can be expressed as follows:

$$\pi_j^\mathbf{x} = \begin{cases} \dfrac{\exp\{\eta_j^\mathbf{x}\}}{\exp\{\eta_1^\mathbf{x}\}+\cdots+\exp\{\eta_{J-1}^\mathbf{x}\}+1} & \text{baseline-category} \\ \dfrac{\exp\{\eta_{J-1}^\mathbf{x}+\cdots+\eta_j^\mathbf{x}\}}{\exp\{\eta_{J-1}^\mathbf{x}+\cdots+\eta_1^\mathbf{x}\}+\exp\{\eta_{J-1}^\mathbf{x}+\cdots+\eta_2^\mathbf{x}\}+\cdots+\exp\{\eta_{J-1}^\mathbf{x}\}+1} & \text{adjacent-categories} \\ \exp\{\eta_j^\mathbf{x}\}\prod_{l=1}^j (\exp\{\eta_l^\mathbf{x}\}+1)^{-1} & \text{continuation-ratio} \end{cases} \tag{S2.2}$$

for $j = 1, \ldots, J-1$ and

$$\pi_J^\mathbf{x} = \begin{cases} \dfrac{1}{\exp\{\eta_1^\mathbf{x}\}+\cdots+\exp\{\eta_{J-1}^\mathbf{x}\}+1} & \text{baseline-category} \\ \dfrac{1}{\exp\{\eta_{J-1}^\mathbf{x}+\cdots+\eta_1^\mathbf{x}\}+\exp\{\eta_{J-1}^\mathbf{x}+\cdots+\eta_2^\mathbf{x}\}+\cdots+\exp\{\eta_{J-1}^\mathbf{x}\}+1} & \text{adjacent-categories} \\ \prod_{l=1}^{J-1} (\exp\{\eta_l^\mathbf{x}\}+1)^{-1} & \text{continuation-ratio} \end{cases}$$

Note that we provide the expression of $\pi_J^\mathbf{x}$ for completeness while $\pi_J^\mathbf{x} = 1 - \pi_1^\mathbf{x} - \cdots - \pi_{J-1}^\mathbf{x}$ is an easier way for numerical calculations.

As for cumulative logit models, the candidate $\mathbf{x}$ must satisfy $-\infty < \eta_1^\mathbf{x} < \eta_2^\mathbf{x} < \cdots < \eta_{J-1}^\mathbf{x} < \infty$. Otherwise, $0 < \pi_j^\mathbf{x} < 1$ might be violated for some $j = 1, \ldots, J$. In other words, the feasible design region should be

$$\mathcal{X}_{\boldsymbol{\theta}} = \{\mathbf{x} \in \mathcal{X} \mid -\infty < \eta_1^\mathbf{x} < \eta_2^\mathbf{x} < \cdots < \eta_{J-1}^\mathbf{x} < \infty\} \tag{S2.3}$$

which depends on the regression parameter $\boldsymbol{\theta}$ (please see Section S.14 in the Supplementary Materials of Bu et al. (2020) for such an example). For cumulative logit models, if $\mathbf{x} \in \mathcal{X}_{\boldsymbol{\theta}}$, then

$$\pi_j^\mathbf{x} = \begin{cases} \dfrac{\exp\{\eta_1^\mathbf{x}\}}{1+\exp\{\eta_1^\mathbf{x}\}} & j = 1 \\ \dfrac{\exp\{\eta_j^\mathbf{x}\}}{1+\exp\{\eta_j^\mathbf{x}\}} - \dfrac{\exp\{\eta_{j-1}^\mathbf{x}\}}{1+\exp\{\eta_{j-1}^\mathbf{x}\}} & 1 < j < J \\ \dfrac{1}{1+\exp\{\eta_{J-1}^\mathbf{x}\}} & j = J \end{cases} \tag{S2.4}$$

according to Lemma S.11 of Bu et al. (2020).

Once $\boldsymbol{\pi}_\mathbf{x} \in \mathbb{R}^J$ is obtained, we can calculate $u_{st}^\mathbf{x} = u_{st}(\boldsymbol{\pi}_\mathbf{x})$ based on Theorem A.2 in Bu et al. (2020) as follows:

(i) $u_{st}^{\mathbf{x}} = u_{ts}^{\mathbf{x}}$, $s, t = 1, \ldots, J$;

(ii) $u_{sJ}^{\mathbf{x}} = 0$ for $s = 1, \ldots, J-1$ and $u_{JJ}^{\mathbf{x}} = 1$;

(iii) For $s = 1, \ldots, J-1$,

$$
u_{ss}^{\mathbf{x}} = \begin{cases}
\pi_s^{\mathbf{x}}(1 - \pi_s^{\mathbf{x}}) & \text{for baseline-category,} \\
(\gamma_s^{\mathbf{x}})^2(1 - \gamma_s^{\mathbf{x}})^2((\pi_s^{\mathbf{x}})^{-1} + (\pi_{s+1}^{\mathbf{x}})^{-1}) & \text{for cumulative,} \\
\gamma_s^{\mathbf{x}}(1 - \gamma_s^{\mathbf{x}}) & \text{for adjacent-categories,} \\
\pi_s^{\mathbf{x}}(1 - \gamma_s^{\mathbf{x}})(1 - \gamma_{s-1}^{\mathbf{x}})^{-1} & \text{for continuation-ratio;}
\end{cases}
$$

(iv) For $1 \le s < t \le J-1$,

$$
u_{st}^{\mathbf{x}} = \begin{cases}
-\pi_s^{\mathbf{x}}\pi_t^{\mathbf{x}} & \text{for baseline-category,} \\
-\gamma_s^{\mathbf{x}}\gamma_t^{\mathbf{x}}(1 - \gamma_s^{\mathbf{x}})(1 - \gamma_t^{\mathbf{x}})(\pi_t^{\mathbf{x}})^{-1} & \text{for cumulative,}\, t - s = 1, \\
0 & \text{for cumulative,}\, t - s > 1, \\
\gamma_s^{\mathbf{x}}(1 - \gamma_t^{\mathbf{x}}) & \text{for adjacent-categories,} \\
0 & \text{for continuation-ratio;}
\end{cases}
$$

where $\gamma_j^{\mathbf{x}} = \pi_1^{\mathbf{x}} + \cdots + \pi_j^{\mathbf{x}}$, $j = 1, \ldots, J-1$; $\gamma_0^{\mathbf{x}} \equiv 0$ and $\gamma_J^{\mathbf{x}} \equiv 1$.

S.3.   Example that $\mathbf{F_x} = \mathbf{F_{x'}}$ with $\mathbf{x} \ne \mathbf{x'}$

Consider a special MLM (3.1) with proportional odds (please see Section S.7 in the Supplementary Materials of Bu et al. (2020) for more technical details). Suppose $d = 2$ and a feasible design point $\mathbf{x} = (x_1, x_2)^T \in [a, b] \times [-c, c] = \mathcal{X}$, $c > 0$, $J \ge 2$, $\mathbf{h}_c(\mathbf{x}) = (x_1, x_2^2)^T$. Then the model matrix at $\mathbf{x} = (x_1, x_2)^T$ is

$$
\mathbf{X_x} = \begin{pmatrix}
1 & 0 & \cdots & 0 & x_1 & x_2^2 \\
0 & 1 & \ddots & \vdots & \vdots & \\
\vdots & \ddots & \ddots & 0 & x_1 & x_2^2 \\
0 & \cdots & 0 & 1 & x_1 & x_2^2 \\
0 & \cdots & 0 & 0 & 0 & 0
\end{pmatrix}_{J \times (J+1)}
$$

Then $p = J + 1$. Let $\boldsymbol{\theta} = (\beta_1, \ldots, \beta_{J-1}, \zeta_1, \zeta_2)^T \in \mathbb{R}^{J-1}$ be the model parameters (since $\boldsymbol{\theta}$ is fixed, we may assume that $\mathcal{X} = \mathcal{X}_{\boldsymbol{\theta}}$ if the model is a cumulative logit model). Let $\mathbf{x'} = (x_1, -x_2)^T$. Then $\mathbf{X_x} = \mathbf{X_{x'}}$ and thus $\boldsymbol{\eta_x} = \boldsymbol{\eta_{x'}}$. According to (S2.2) (or (S2.4)), we obtain $\boldsymbol{\pi_x} = \boldsymbol{\pi_{x'}}$ and then $\mathbf{U_x} = \mathbf{U_{x'}}$. The Fisher information matrix at $\mathbf{x}$ is $\mathbf{F_x} = \mathbf{X_x}^T \mathbf{U_x} \mathbf{X_x} = \mathbf{X_{x'}}^T \mathbf{U_{x'}} \mathbf{X_{x'}} = \mathbf{F_{x'}}$. Note that $\mathbf{x} \ne \mathbf{x'}$ if $x_2 \ne 0$.

S.4.   First-order derivative of sensitivity function

As mentioned in Section 3.1, to apply Algorithm 1 for MLM, we need to calculate the first-order derivative of the sensitivity function $d(\mathbf{x}, \boldsymbol{\xi})$.

Recall that the first k ($1 \le k \le d$) factors are continuous. Given $\mathbf{x} = (x_1, \ldots, x_d)^T \in \mathcal{X}$, for each $i = 1, \ldots, k$, according to Formulae 17.1(a), 17.2(a) and 17.7 in Seber (2008),

$$
\begin{aligned}
\frac{\partial d(\mathbf{x}, \boldsymbol{\xi})}{\partial x_i} &= \frac{\partial \mathrm{tr}(\mathbf{F}(\boldsymbol{\xi})^{-1}\mathbf{F}_\mathbf{x})}{\partial x_i} = \mathrm{tr}\left(\mathbf{F}(\boldsymbol{\xi})^{-1}\frac{\partial \mathbf{F}_\mathbf{x}}{\partial x_i}\right) \\
&= \mathrm{tr}\left(\mathbf{F}(\boldsymbol{\xi})^{-1}\left[\frac{\partial \mathbf{X}_\mathbf{x}^T}{\partial x_i}\mathbf{U}_\mathbf{x}\mathbf{X}_\mathbf{x} + \mathbf{X}_\mathbf{x}^T\frac{\partial \mathbf{U}_\mathbf{x}}{\partial x_i}\mathbf{X}_\mathbf{x} + \mathbf{X}_\mathbf{x}^T\mathbf{U}_\mathbf{x}\frac{\partial \mathbf{X}_\mathbf{x}}{\partial x_i}\right]\right)
\end{aligned}
\tag{S4.5}
$$

where

$$
\frac{\partial \mathbf{X}_\mathbf{x}}{\partial x_i} = \begin{pmatrix}
\frac{\partial \mathbf{h}_1^T(\mathbf{x})}{\partial x_i} & \mathbf{0}^T & \cdots & \mathbf{0}^T & \frac{\partial \mathbf{h}_c^T(\mathbf{x})}{\partial x_i} \\
\mathbf{0}^T & \frac{\partial \mathbf{h}_2^T(\mathbf{x})}{\partial x_i} & \ddots & \vdots & \vdots \\
\vdots & \ddots & \ddots & \mathbf{0}^T & \frac{\partial \mathbf{h}_c^T(\mathbf{x})}{\partial x_i} \\
\mathbf{0}^T & \cdots & \mathbf{0}^T & \frac{\partial \mathbf{h}_{J-1}^T(\mathbf{x})}{\partial x_i} & \frac{\partial \mathbf{h}_c^T(\mathbf{x})}{\partial x_i} \\
\mathbf{0}^T & \cdots & \cdots & \mathbf{0}^T & \mathbf{0}^T
\end{pmatrix}_{J \times p}
\tag{S4.6}
$$

and $\frac{\partial \mathbf{U}_\mathbf{x}}{\partial x_i} = \left(\frac{\partial u_{st}^\mathbf{x}}{\partial x_i}\right)_{s,t=1,\ldots,J}$ with

$$
\frac{\partial u_{st}^\mathbf{x}}{\partial x_i} = \frac{\partial u_{st}^\mathbf{x}}{\partial \boldsymbol{\pi}_\mathbf{x}^T} \cdot \frac{\partial \boldsymbol{\pi}_\mathbf{x}}{\partial \boldsymbol{\eta}_\mathbf{x}^T} \cdot \frac{\partial \boldsymbol{\eta}_\mathbf{x}}{\partial x_i} = \frac{\partial u_{st}^\mathbf{x}}{\partial \boldsymbol{\pi}_\mathbf{x}^T} \cdot \left(\mathbf{C}^T\mathbf{D}_\mathbf{x}^{-1}\mathbf{L}\right)^{-1} \cdot \frac{\partial \mathbf{X}_\mathbf{x}}{\partial x_i} \cdot \boldsymbol{\theta}
\tag{S4.7}
$$

with $\mathbf{C}$ and $\mathbf{L}$ defined as in (3.1), and $\mathbf{D}_\mathbf{x} = \mathrm{diag}(\mathbf{L}\boldsymbol{\pi}_\mathbf{x})$. Explicit formula of $(\mathbf{C}^T\mathbf{D}_\mathbf{x}^{-1}\mathbf{L})^{-1}$ can be found in Section S.3 in the Supplementary Materials of Bu et al. (2020) with $\mathbf{x}_i$ replaced by $\mathbf{x}$. As for $\frac{\partial u_{st}^\mathbf{x}}{\partial \boldsymbol{\pi}_\mathbf{x}^T}$, we have the following explicit formulae

(i) $\frac{\partial u_{st}^\mathbf{x}}{\partial \boldsymbol{\pi}_\mathbf{x}} = \frac{\partial u_{ts}^\mathbf{x}}{\partial \boldsymbol{\pi}_\mathbf{x}}$, $s, t = 1, \ldots, J$;

(ii) $\frac{\partial u_{s,J}^\mathbf{x}}{\partial \boldsymbol{\pi}_\mathbf{x}} = \mathbf{0} \in \mathbb{R}^J$ for $s = 1, \ldots, J$;

(iii) For $s = 1, \ldots, J-1$,

$$
\frac{\partial u_{ss}^\mathbf{x}}{\partial \boldsymbol{\pi}_\mathbf{x}} = \begin{cases}
\left(\pi_s^\mathbf{x}\mathbf{1}_{s-1}^T, 1 - \pi_s^\mathbf{x}, \pi_s^\mathbf{x}\mathbf{1}_{J-s}^T\right)^T & \text{for baseline-category} \\
u_{ss}^\mathbf{x}\left[\left(\frac{2}{\gamma_s^\mathbf{x}}\mathbf{1}_s^T, \frac{2}{1-\gamma_s^\mathbf{x}}\mathbf{1}_{J-s}^T\right)^T \right. & \\
\left. -\frac{\pi_{s+1}^\mathbf{x}\mathbf{e}_s}{\pi_s^\mathbf{x}(\pi_s^\mathbf{x}+\pi_{s+1}^\mathbf{x})} - \frac{\pi_s^\mathbf{x}\mathbf{e}_{s+1}}{\pi_{s+1}^\mathbf{x}(\pi_s^\mathbf{x}+\pi_{s+1}^\mathbf{x})}\right] & \text{for cumulative} \\
\left((1 - \gamma_s^\mathbf{x})\mathbf{1}_s^T, \gamma_s^\mathbf{x}\mathbf{1}_{J-s}^T\right)^T & \text{for adjacent-categories} \\
\left(\mathbf{0}_{s-1}^T, \frac{(1-\gamma_s^\mathbf{x})^2}{(1-\gamma_{s-1}^\mathbf{x})^2}, \frac{(\pi_s^\mathbf{x})^2\mathbf{1}_{J-s}^T}{(1-\gamma_{s-1}^\mathbf{x})^2}\right)^T & \text{for continuation-ratio}
\end{cases}
$$

where $\mathbf{e}_s$ is the $J \times 1$ vector with the sth coordinate 1 and all others 0, $\mathbf{1}_s$ is the $s \times 1$ vector of all 1, and $\mathbf{0}_s$ is the $s \times 1$ vector of all 0.

(iv) For $1 \leq s < t \leq J - 1$,

$$\frac{\partial u_{st}^{\mathbf{x}}}{\partial \boldsymbol{\pi}_{\mathbf{x}}} = \begin{cases} \left(\mathbf{0}_{s-1}^T, -\pi_t^{\mathbf{x}}, \mathbf{0}_{t-s-1}^T, -\pi_s^{\mathbf{x}}, \mathbf{0}_{J-t}^T\right)^T & \text{for baseline-category} \\ \left(-(1-\gamma_s^{\mathbf{x}})(1-\gamma_t^{\mathbf{x}})\left(1 + \frac{2\gamma_s^{\mathbf{x}}}{\pi_t^{\mathbf{x}}}\right)\mathbf{1}_s^T, \right. \\ \quad -\gamma_s^{\mathbf{x}}(1-\gamma_t^{\mathbf{x}})\left[1 - \frac{\gamma_s^{\mathbf{x}}(1-\gamma_t^{\mathbf{x}})}{(\pi_t^{\mathbf{x}})^2}\right], \\ \quad \left. -\gamma_s^{\mathbf{x}}\gamma_t^{\mathbf{x}}\left[1 + \frac{2(1-\gamma_t^{\mathbf{x}})}{\pi_t}\right]\mathbf{1}_{J-s-1}^T\right)^T & \text{for cumulative}, t-s=1 \\ \mathbf{0}_J & \text{for cumulative}, t-s>1 \\ \left((1-\gamma_t^{\mathbf{x}})\mathbf{1}_s^T, \mathbf{0}_{t-s}^T, \gamma_s^{\mathbf{x}}\mathbf{1}_{J-t}^T\right)^T & \text{for adjacent-categories} \\ \mathbf{0}_J & \text{for continuation-ratio} \end{cases}$$

where $\gamma_j^{\mathbf{x}} = \pi_1^{\mathbf{x}} + \cdots + \pi_j^{\mathbf{x}}$, $j = 1, \ldots, J-1$; $\gamma_0^{\mathbf{x}} \equiv 0$ and $\gamma_J^{\mathbf{x}} \equiv 1$.

Thus the explicit formulae for $\frac{\partial d(\mathbf{x}, \boldsymbol{\xi})}{\partial x_i}$, $i = 1, \ldots, k$ can be obtained via (S4.5). Only $\frac{\partial \mathbf{X}_{\mathbf{x}}}{\partial x_i}$ is related to i, which will speed up the computations.

S.5. Technical details of house flies example

In this section, we follow Section 3.2 and provide more technical details of the ForLion algorithm for the emergence of house flies example. To use our ForLion algorithm, $p_1 = 3$, $p_2 = 2$, $p_c = 0$, and $p = p_1 + p_2 + p_c = 5$. Given $\mathbf{x} = x \in \mathcal{X} = [80, 200]$ or $[0, 200]$, we have $\mathbf{h}_1(\mathbf{x}) = (1, x, x^2)^T$, $\mathbf{h}_2(\mathbf{x}) = (1, x)^T$, $\mathbf{h}_c(\mathbf{x}) = 0$. Correspondingly,

$$\mathbf{X}_{\mathbf{x}} = \begin{pmatrix} 1 & x & x^2 & 0 & 0 \\ 0 & 0 & 0 & 1 & x \\ 0 & 0 & 0 & 0 & 0 \end{pmatrix}_{3\times 5}, \quad \frac{\partial \mathbf{X}_{\mathbf{x}}}{\partial x} = \begin{pmatrix} 0 & 1 & 2x & 0 & 0 \\ 0 & 0 & 0 & 0 & 1 \\ 0 & 0 & 0 & 0 & 0 \end{pmatrix}_{3\times 5}$$

and $\boldsymbol{\eta}^{\mathbf{x}} = \mathbf{X}_{\mathbf{x}}\boldsymbol{\theta} = (\beta_{11} + \beta_{12}x + \beta_{13}x^2, \beta_{21} + \beta_{22}x, 0)^T$. To calculate $\mathbf{F}_{\mathbf{x}} = \mathbf{X}_{\mathbf{x}}^T \mathbf{U}_{\mathbf{x}} \mathbf{X}_{\mathbf{x}}$, we also need

$$\mathbf{U}_{\mathbf{x}} = \begin{pmatrix} \frac{\pi_1^{\mathbf{x}}(1-\gamma_1^{\mathbf{x}})}{1-\gamma_0^{\mathbf{x}}} & 0 & 0 \\ 0 & \frac{\pi_2^{\mathbf{x}}(1-\gamma_2^{\mathbf{x}})}{1-\gamma_1^{x}} & 0 \\ 0 & 0 & 1 \end{pmatrix}_{3\times 3}$$

with $\gamma_0^{\mathbf{x}} = 0$, $\gamma_1^{\mathbf{x}} = \pi_1^{\mathbf{x}}$, $\gamma_2^{\mathbf{x}} = \pi_1^{\mathbf{x}} + \pi_2^{\mathbf{x}}$.

For Step $5°$ of the ForLion algorithm, we have $k = d = 1$. To use the R function `optim` with option "L-BFGS-B" (a quasi-Newton method), we need to calculate $\frac{\partial d(\mathbf{x}, \boldsymbol{\xi}_t)}{\partial x}$ based on (S4.5) and (S4.7), where $\frac{\partial u_{s3}^{\mathbf{x}}}{\partial \boldsymbol{\pi}_{\mathbf{x}}^T} = \frac{\partial u_{3s}^{\mathbf{x}}}{\partial \boldsymbol{\pi}_{\mathbf{x}}^T} = (0,0,0)$ for $s = 1, 2, 3$; $\frac{\partial u_{11}^{\mathbf{x}}}{\partial \boldsymbol{\pi}_{\mathbf{x}}^T} = ((1-\gamma_1^{\mathbf{x}})^2, (\pi_1^{\mathbf{x}})^2, (\pi_1^{\mathbf{x}})^2)$; $\frac{\partial u_{22}^{\mathbf{x}}}{\partial \boldsymbol{\pi}_{\mathbf{x}}^T} = (0, \frac{(1-\gamma_2^{\mathbf{x}})^2}{(1-\gamma_1^{\mathbf{x}})^2}, \frac{(\pi_2^{\mathbf{x}})^2}{(1-\gamma_1^{\mathbf{x}})^2})$; $\frac{\partial u_{12}^{\mathbf{x}}}{\partial \boldsymbol{\pi}_{\mathbf{x}}^T} = \frac{\partial u_{21}^{\mathbf{x}}}{\partial \boldsymbol{\pi}_{\mathbf{x}}^T} = (0,0,0)$; and

$$(\mathbf{C}^T \mathbf{D}_{\mathbf{x}}^{-1} \mathbf{L})^{-1} = \begin{pmatrix} \pi_1^{\mathbf{x}}(1-\gamma_1^{\mathbf{x}}) & 0 & \pi_1^{\mathbf{x}} \\ -\pi_1^{\mathbf{x}}\pi_2^{\mathbf{x}} & \frac{\pi_2^{\mathbf{x}}(1-\gamma_2^{\mathbf{x}})}{1-\gamma_1^{\mathbf{x}}} & \pi_2^{\mathbf{x}} \\ -\pi_1^{\mathbf{x}}\pi_3^{\mathbf{x}} & -\frac{\pi_2^{\mathbf{x}}\pi_3^{\mathbf{x}}}{1-\gamma_1^{\mathbf{x}}} & \pi_3^{\mathbf{x}} \end{pmatrix}_{3\times 3}$$

Factor (Unit, Parameter)	Factor Levels/Range	Parameter Nominal Value	Parameter Prior Distribution
Cleaning Method (β_1)	CM_2, CM_3	-0.970	$U(-1, 0)$
Deposition temperature (°C, β_2)	$[-25, 25]$	0.077	$U(0, 0.2)$
Deposition pressure (mtorr, β_3)	$[-200, 200]$	0.008	$U(-0.1, 0.1)$
Nitrogen flow (seem, β_4)	$[-150, 0]$	-0.007	$U(-0.1, 0.1)$
Silane flow (seem, β_5)	$[-100, 0]$	0.007	$U(-0.1, 0.1)$
Settling time (min, β_6)	$[0, 16]$	0.056	$U(0, 0.2)$
Cut point 1 (θ_1)	(Intercept)	-1.113	$U(-2, -1)$
Cut point 2 (θ_2)	(Intercept)	0.183	$U(-0.5, 0.5)$
Cut point 3 (θ_3)	(Intercept)	1.518	$U(1, 2)$
Cut point 4 (θ_4)	(Intercept)	2.639	$U(2.5, 3.5)$

Table S.1: Factors/parameters in the example of minimizing surface defects

S.6. Example: Minimizing surface defects

In Chapter 4 of Phadke (1989), a polysilicon deposition process for manufacturing very large scale integrated (VLSI) circuits was described with six control factors, Deposition temperature (°C), Deposition pressure (mtorr), Nitrogen flow rate (seem), Silane flow rate (seem), and Settling time (minutes). Wu (2008) used the relevant experiment as an illustrative example and categorized the response Surface Defects from a count number to one of the five ordered categories, Practically no surface defects (I, $0 \sim 3$), Very few defects (II, $4 \sim 30$), Some defects (III, $31 \sim 300$), Many defects (IV, $301 \sim 1000$), and Too many defects (V, 1001 and above). Lukemire et al. (2022) utilized this experiment as an example under a cumulative logit model with po and interpreted the factor Cleaning Method as binary and the other five control factors as continuous ones. The levels and ranges of these factors are listed in Table S.1 (see also Table 6 in Lukemire et al. (2022)).

In our notations, the cumulative logit model used by Lukemire et al. (2022) for the surface defects experiment can be expressed as follows:

$$\log \left(\frac{\pi_{i1} + \cdots + \pi_{ij}}{\pi_{i,j+1} + \cdots + \pi_{iJ}} \right) = \theta_j - \beta_1 x_{i1} - \beta_2 x_{i2} - \beta_3 x_{i3} - \beta_4 x_{i4} - \beta_5 x_{i5} - \beta_6 x_{i6} \quad \text{(S6.8)}$$

with $i = 1, \ldots, m$ and $j = 1, 2, 3, 4$.

In this example, $d = 6$, $k = 5$, $p = 10$, and $\boldsymbol{\theta} = (\theta_1, \theta_2, \theta_3, \theta_4, \beta_1, \beta_2, \beta_3, \beta_4, \beta_5, \beta_6)^T$. Given $\mathbf{x} = (x_1, x_2, x_3, x_4, x_5, x_6)^T$, $\mathbf{h}_1^T(\mathbf{x}) = \cdots = \mathbf{h}_4^T(\mathbf{x}) \equiv 1$, $\mathbf{h}_c^T(\mathbf{x}) \equiv \mathbf{x}$.

We compare the performance of the PSO algorithm described in Lukemire et al. (2022), Bu et al. (2020)'s lift-one algorithm on grid points, and our ForLion algorithm by a simulation study. For the PSO algorithm, following Lukemire et al. (2022), we use 24 support points and 20 particles with up to $50,000$ maximum iterations. For Bu et al. (2020)'s lift-one algorithm, we use grid lengths 2 and 3, respectively, for discretizing the five continuous factors, which means that we use 2 or 3 equally spaced points within the ranges of each continuous factor to obtain the grid points. The corresponding design space consists of $2 \times 2^5 = 64$ or $2 \times 3^5 = 486$ design points, respectively. Grids with a length 4 or more are skipped in this case due to extremely long running time. For the ForLion algorithm, we use merging threshold $\delta = 0.2$ and converging threshold $\epsilon = 10^{-6}$
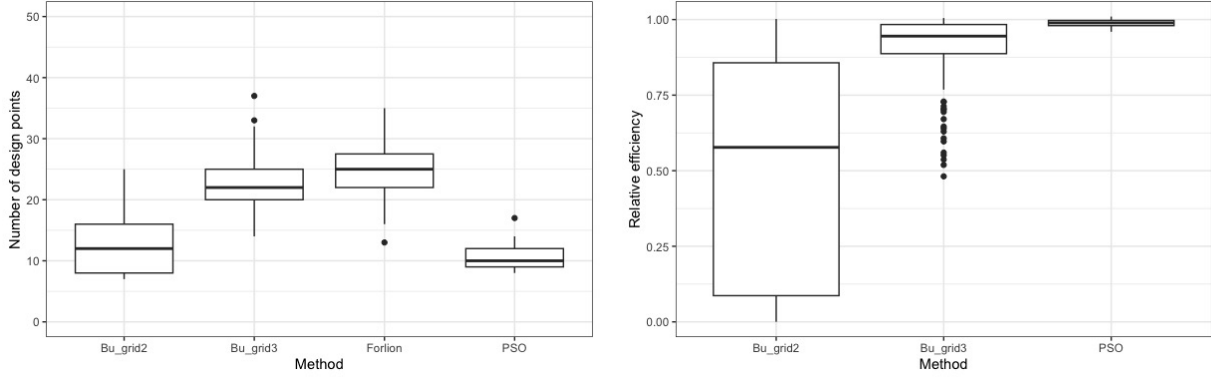
(a) Number of design points	(b) Relative efficiency w.r.t. ForLion

Figure S.1: Boxplots of 100 simulations for Bu's, ForLion, and PSO algorithms on the surface defects study with five categories

for illustration. Both ForLion and Bu's algorithms are written in R, while PSO's is implemented in Julia. We randomly simulate 100 parameter vectors from the uniform distributions listed in Table S.1 as the assumed true values, respectively. Figure S.1 shows the numbers of design points of Bu's Grid-2, Bu's Grid-3, ForLion, PSO designs and their relative efficiencies with respect to the ForLion designs. The median numbers of the design points of the constructed designs are 10 for PSO, 12 for Bu's Grid-2, 22 for Bu's Grid-3, and 25 for ForLion. The average of relative efficiencies compared to ForLion's, defined as $[f(\boldsymbol{\xi})/f(\boldsymbol{\xi}_{\mathrm{ForLion}})]^{1/10}$, are 49.12% for Bu's Grid-2, 89.38% for Bu's Grid-3, and 98.82% for PSO. The median running time on the desktop described in Section 3.2 is 0.95s for Bu's Grid-2, 433.8s for Bu's Grid-3, 25.50s for PSO, and 146.83s for ForLion.

As a conclusion, Bu et al. (2020)'s lift-one algorithm with grid points does not work well for this case with five continuous factors. Neither Grid-2 nor Grid-3 has satisfactory relative efficiencies, while Grid-4 or above is computationally too heavy. PSO algorithm in this case has again the advantages on reduced computational time and numbers of design points. The advantage of the ForLion algorithm is that its relative efficiencies are apparently higher than PSO's, although the improvement is not as impressive as in the electrostatic discharge experiment (see Example 3).

To check whether the improvement of the ForLion's designs against PSO's in terms of relative efficiency is significant, we test if the mean relative efficiency is significantly less than 1. Supported by the Box-Cox Transformations (Box and Cox, 1964; Venables and Ripley, 2002), we run a one-sided t-test to check if $f(\boldsymbol{\xi}_{\mathrm{PSO}})/f(\boldsymbol{\xi}_{\mathrm{ForLion}})$ is equal to or less than 1. The p-value $< 2.2 \times 10^{-16}$ suggests that the ratio is significantly less than 1. Actually, a 95% confidence interval for $f(\boldsymbol{\xi}_{\mathrm{PSO}})/f(\boldsymbol{\xi}_{\mathrm{ForLion}})$ is $(0.873, 0.915)$. That is, from the optimization point of view, the maximum value of the objective function $f(\boldsymbol{\xi})$ achieved by PSO is only about 90% on average of the one achieved by ForLion in this case.

S.7. Fisher information matrix for GLMs

In this section, we provide the details of the Fisher information matrix for the GLM (4.3). The number of covariates d could be much less than the number of parameters p. For example, for an experiment with $d = 3$ factors x_1, x_2, x_3, the model $g(E(Y)) = \beta_0 + \beta_1 x_1 + \beta_2 x_2 + \beta_3 x_3 + \beta_4 x_1 x_2$ contains $p = 5$ parameters which covers the intercept and an interaction term $x_1 x_2$.

Assuming that there are m distinct covariate combinations $\mathbf{x}_1, \ldots, \mathbf{x}_m$ with the numbers of replicates $n_1, \ldots, n_m$, respectively, where $n_1 + \cdots + n_m = n$. The Fisher information matrix $\mathbf{F}$ can be written as (Yang and Mandal, 2015)

$$\mathbf{F} = n\mathbf{X}^T\mathbf{W}\mathbf{X} = n\sum_{i=1}^{m} w_i \nu_i \mathbf{X}_i \mathbf{X}_i^T \tag{S7.9}$$

where $\mathbf{X} = (\mathbf{X}_1, \ldots, \mathbf{X}_m)^T$ is an $m \times p$ matrix, known as the model matrix, and $\mathbf{W} = \mathrm{diag}\{w_1\nu_1, \ldots, w_m\nu_m\}$ is an $m \times m$ diagonal matrix with $w_i = n_i/n$ and

$$\nu_i = \frac{1}{\mathrm{Var}(Y_i)}\left(\frac{\partial \mu_i}{\partial \eta_i}\right)^2$$

Here w_i is the proportion of experimental units assigned to the design point $\mathbf{x}_i$ and ν_i represents how much information the design point $\mathbf{x}_i$ could provide.

For typical applications, the link function g is one-to-one and differentiable. Following Yang and Mandal (2015), we assume that $E(Y)$ itself determines $\mathrm{Var}(Y)$. Then there exists a function s such that $\mathrm{Var}(Y_i) = s(\eta_i)$. Let $\nu = \left[(g^{-1})'\right]^2/s$. Then $\nu_i = \nu(\eta_i) = \nu\left(\mathbf{X}_i^T\boldsymbol{\beta}\right)$ for each $i = 1, \ldots, m$. Please see Table 5 in the Supplementary Materials of Huang et al. (2023) for some examples of the function ν (see also McCullagh and Nelder (1989); Christensen (2015); Yang and Mandal (2015)). Besides, according to Liu (2004), the t link family $g(\mu) = F_\nu^{-1}(\mu)$ incorporates logit and probit links approximately, where F_ν is the cumulative distribution function of t distribution with degrees of freedom $\nu > 0$. In Section S.1, we provide more formulae including $\nu'(\eta)$'s, which are needed for the ForLion algorithm (see also Section S.8 in the Supplementary Material).

S.8. First-order derivative of sensitivity function for GLMs

In this section, similar as in Section S.4, to search for the new design point $\mathbf{x}^*$ in Step 5° of Algorithm 1, we provide the first-order derivatives of $d(\mathbf{x}, \boldsymbol{\xi}_t)$ for GLMs, given $\mathbf{x} = (x_1, \ldots, x_d)^T \in \mathcal{X}$. Recall that the first k factors are continuous with $x_i \in [a_i, b_i]$ and the last $d - k$ factors are discrete with $x_i \in I_i$, $1 \leq k \leq d$. Denote $\mathbf{x}_{(1)} = (x_1, \ldots, x_k)^T$. To simplify the notations, we denote $\mathbf{A} = (\mathbf{X}_{\boldsymbol{\xi}_t}^T \mathbf{W}_{\boldsymbol{\xi}_t} \mathbf{X}_{\boldsymbol{\xi}_t})^{-1}$, which is a known positive definite matrix given $\boldsymbol{\xi}_t$ and $\boldsymbol{\beta}$. To perform the quasi-Newton method for Step 5° of

Algorithm 1, we need the partial gradient as follows

$$
\begin{aligned}
\frac{\partial d(\mathbf{x}, \boldsymbol{\xi}_t)}{\partial \mathbf{x}_{(1)}} &= \nu'(\boldsymbol{\beta}^T \mathbf{h}(\mathbf{x})) \cdot \mathbf{h}(\mathbf{x})^T \mathbf{A} \mathbf{h}(\mathbf{x}) \cdot \left[\frac{\partial \mathbf{h}(\mathbf{x})}{\partial \mathbf{x}_{(1)}^T} \right]^T \boldsymbol{\beta} \\
&+ 2 \cdot \nu(\boldsymbol{\beta}^T \mathbf{h}(\mathbf{x})) \cdot \left[\frac{\partial \mathbf{h}(\mathbf{x})}{\partial \mathbf{x}_{(1)}^T} \right]^T \mathbf{A} \mathbf{h}(\mathbf{x})
\end{aligned}
$$

where $\partial \mathbf{h}(\mathbf{x}) / \partial \mathbf{x}_{(1)}^T$ is a $p \times k$ matrix. Note that in general $d(\mathbf{x}, \boldsymbol{\xi}_t)$ is not a convex function of $\mathbf{x}$ or $\mathbf{x}_{(1)}$. Typically when $k \geq 2$, we need to try multiple initial $\mathbf{x}_{(1)}$'s to bridge the gap between the local maximum and global maximum.

To facilitate the readers, we provide the formulae of $\nu(\eta)$ and $\nu'(\eta)$ for commonly used GLMs in Section S.1.

S.9. GLMs with main-effects continuous factors

In this section, we provide the formulae for a special class of GLMs with mixed factors, whose continuous factors are involved as main-effects only. That is, we assume that the predictors $\mathbf{h}(\mathbf{x}) = (h_1(\mathbf{x}), \ldots, h_p(\mathbf{x}))^T$ satisfy $h_i(\mathbf{x}) = x_i$ for $i = 1, \ldots, k$ and $h_{k+1}(\mathbf{x}), \ldots, h_p(\mathbf{x})$ do not depend on the continuous factors $x_1, \ldots, x_k$. In other words, the linear predictor of the GLM model takes the form of

$$
\eta = \beta_1 x_1 + \cdots + \beta_k x_k + \beta_{k+1} h_{k+1}(\mathbf{x}_{(2)}) + \cdots + \beta_p h_p(\mathbf{x}_{(2)}) \tag{S9.10}
$$

where $\mathbf{x}_{(2)} = (x_{k+1}, \ldots, x_d)^T$. Note that $h_{k+1}(\mathbf{x}_{(2)})$ could be 1 and then β_{k+1} represents the intercept.

Recall that $\mathbf{x} = (\mathbf{x}_{(1)}^T, \mathbf{x}_{(2)}^T)^T$ and $\mathbf{x}_{(1)} = (x_1, \ldots, x_k)^T$. We denote $\boldsymbol{\beta}_{(1)} = (\beta_1, \ldots, \beta_k)^T$, $\boldsymbol{\gamma}_{(1)} = (\gamma_1, \ldots, \gamma_k)^T$, and $\mathbf{A}_{11}$ as the kth leading principle submatrix of $\mathbf{A} = (\mathbf{X}_{\boldsymbol{\xi}_t}^T \mathbf{W}_{\boldsymbol{\xi}_t} \mathbf{X}_{\boldsymbol{\xi}_t})^{-1}$, that is, the $k \times k$ submatrix of $\mathbf{A}$ formed by the first k rows and the first k columns.

In this case, the $p \times k$ matrix $\partial \mathbf{h}(\mathbf{x}) / \partial \mathbf{x}_{(1)}^T = (\mathbf{I}_k \ \mathbf{0})^T$, the $k \times k$ matrix $\partial^2 h_i(\mathbf{x}) / (\partial \mathbf{x}_{(1)} \partial \mathbf{x}_{(1)}^T) = \mathbf{0}$ for $i = 1, \ldots, p$, and

$$
\left[\frac{\partial \mathbf{h}(\mathbf{x})}{\partial \mathbf{x}_{(1)}^T} \right]^T \boldsymbol{\beta} = \boldsymbol{\beta}_{(1)}, \quad \left[\frac{\partial \mathbf{h}(\mathbf{x})}{\partial \mathbf{x}_{(1)}^T} \right]^T \mathbf{A} \mathbf{h}(\mathbf{x}) = \boldsymbol{\gamma}_{(1)}
$$

Therefore, the partial gradient in this case is

$$
\frac{\partial d(\mathbf{x}, \boldsymbol{\xi}_t)}{\partial \mathbf{x}_{(1)}} = \nu'(\boldsymbol{\beta}^T \mathbf{h}(\mathbf{x})) \cdot \mathbf{h}(\mathbf{x})^T \mathbf{A} \mathbf{h}(\mathbf{x}) \cdot \boldsymbol{\beta}_{(1)} + 2 \cdot \nu(\boldsymbol{\beta}^T \mathbf{h}(\mathbf{x})) \cdot \boldsymbol{\gamma}_{(1)}
$$

The formulae in this section are helpful for examples in Section 4.3.

S.10. Electrostatic discharge example supplementary

In this section, we provide more details about Example 3 on the electrostatic discharge experiment.

Table S.2: Designs Obtained for Example 3

	Lukemire et al. (2019)'s $\boldsymbol{\xi}_o$						ForLion's $\boldsymbol{\xi}_*$					
i	A	B	ESD	Pulse	Volt.	$w_i(\%)$	A	B	ESD	Pulse	Volt.	$w_i(\%)$
1	-1	-1	-1	-1	25.00	7.46	-1	-1	-1	-1	25.00	7.49
2	-1	-1	-1	-1	28.04	1.80	-1	-1	-1	-1	27.55	1.56
3	-1	-1	-1	1	25.00	2.49	-1	-1	-1	1	25.00	3.66
4	-1	-1	-1	1	27.85	7.74	-1	-1	-1	1	28.69	7.22
5	-1	-1	1	-1	25.00	11.65	-1	-1	1	-1	25.00	11.65
6	-1	-1	1	1	25.00	8.58	-1	-1	1	1	25.00	8.54
7	-1	1	-1	-1	25.00	9.20	-1	1	-1	-1	25.00	8.95
8	–	–	–	–	–	–	-1	1	-1	-1	29.06	0.42
9	-1	1	-1	1	25.00	10.00	-1	1	-1	1	25.00	10.08
10	-1	1	1	-1	25.00	3.80	-1	1	1	-1	25.00	3.41
11	-1	1	1	-1	32.93	13.43	-1	1	1	-1	32.78	13.13
12	-1	1	1	1	25.00	9.20	-1	1	1	1	25.00	9.23
13	1	-1	1	-1	25.00	1.23	1	-1	1	-1	25.00	1.36
14	1	1	1	-1	25.00	13.40	1	1	1	-1	25.00	13.31

Table S.2 shows the 14-points design obtained from the Forlion algorithm and 13-points design from Lukemire et al. (2019) (see Section 4.3). They are fairly close to each other. As mentioned in Example 3, ForLion's $\boldsymbol{\xi}_*$ is slightly more efficient.

We also conduct a simulation study on Example 3 to examine the effect of the merging threshold δ in Step 2° of Algorithm 1. In the study, we assume that $\boldsymbol{\theta} = (\beta_0, \beta_1, \beta_2, \beta_3, \beta_4, \beta_5, \beta_{34})^T = (-7.84, 1.14, -0.21, 0, 0.38, 0.27, 0.45)^T$ are the true parameter values. We apply the ForLion algorithm to find D-optimal designs with different merging thresholds $\delta \in \{0.005, 0.01, 0.02, 0.03, 0.04, 0.05\}$. The results are shown in Figure S.2. We can see that: (1) The number of design points decreases as we increase the merging threshold δ, from 29 when $\delta = 0.005$ to 21 when $\delta = 0.02$, and it then stabilizes at 20 when $\delta \geq 0.03$; (2) the relative efficiency with respect to the design with $\delta = 0.005$ remains around 100%; (3) the minimum distance among design points increases along with δ; (4) the running time roughly shows a decreasing pattern with the minimum occurs at $\delta = 0.03$ or $\delta = 0.05$. Overall we choose $\delta = 0.03$ for the simulation study described in Example 3.

S.11.   Proofs

Proof of Theorem 1: As a direct conclusion of Theorem 2.2 of Fedorov and Leonov (2014), under regularity conditions, there exists a D-optimal design that contains no more than $p(p + 1)/2$ support points, which are the design points with positive weights.

According to Theorem 2.2 of Fedorov and Leonov (2014), a design $\boldsymbol{\xi}$ is optimal if and only if $\min_{\mathbf{x} \in \mathcal{X}} \psi(\mathbf{x}, \boldsymbol{\xi}) \geq 0$. Under D-criterion, it is equivalent to $\max_{\mathbf{x} \in \mathcal{X}} d(\mathbf{x}, \boldsymbol{\xi}) \leq p$ in our notations. If a design $\boldsymbol{\xi}$ is reported by Algorithm 1, it must satisfy $\max_{\mathbf{x} \in \mathcal{X}} d(\mathbf{x}, \boldsymbol{\xi}) \leq p$ and thus be D-optimal. $\square$

Proof of Theorem 2: It is a direct conclusion of Corollary 3.1 of Bu et al. (2020), $\mathbf{F_x} = \mathbf{X_x}^T \mathbf{U_x} \mathbf{X_x}$, where $\mathbf{U_x} = (u_{st}^{\mathbf{x}})_{s,t=1,...,J}$. $\square$
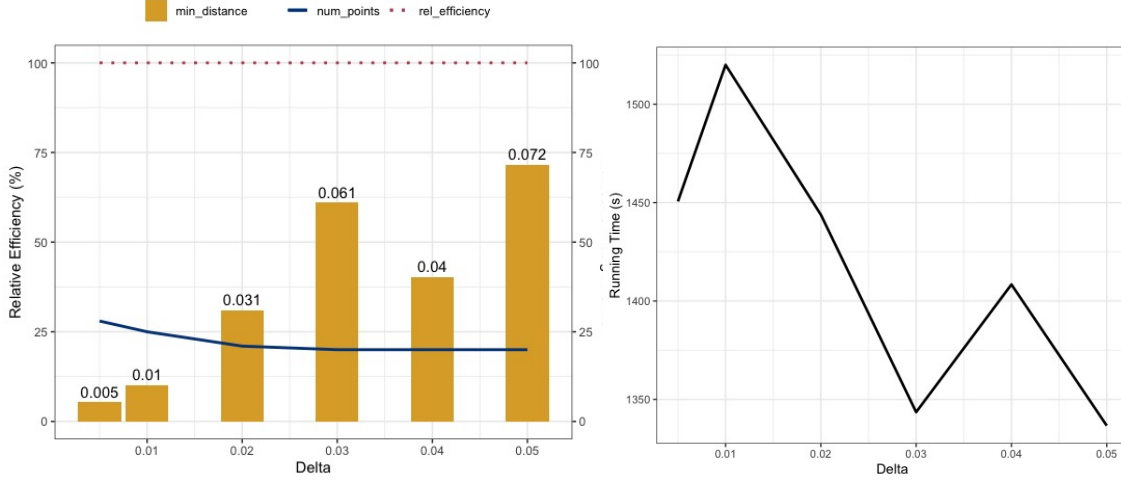
(a) Number of design points, minimum distance among design points, and relative efficiency w.r.t. the design with $\delta = 0.005$

(b) Running time

Figure S.2: Simulation results of ForLion algorithm with merging threshold $\delta \in \{0.05, 0.01, 0.02, 0.03, 0.04, 0.05\}$

Lemma 1. *Let*

$$\mathbf{A} = \begin{bmatrix} \mathbf{A}_{11} & \cdots & \mathbf{A}_{1J} \\ \vdots & \ddots & \vdots \\ \mathbf{A}_{J1} & \cdots & \mathbf{A}_{JJ} \end{bmatrix}, \quad \mathbf{B} = \begin{bmatrix} \mathbf{B}_{11} & \cdots & \mathbf{B}_{1J} \\ \vdots & \ddots & \vdots \\ \mathbf{B}_{J1} & \cdots & \mathbf{B}_{JJ} \end{bmatrix}$$

be two $n \times n$ symmetric matrices with submatrices $\mathbf{A}_{ij}, \mathbf{B}_{ij} \in \mathbb{R}^{n_i \times n_j}$, $i, j = 1, \ldots, J$, $\sum_{i=1}^{J} n_i = n$. Then

$$\mathrm{tr}(\mathbf{A}\mathbf{B}) = \sum_{i=1}^{J} \sum_{j=1}^{J} \mathrm{tr}(\mathbf{A}_{ij}\mathbf{B}_{ij}^T) = \sum_{j=1}^{J} \mathrm{tr}(\mathbf{A}_{jj}\mathbf{B}_{jj}) + 2 \sum_{i=1}^{J-1} \sum_{j=i+1}^{J} \mathrm{tr}(\mathbf{A}_{ij}\mathbf{B}_{ij}^T)$$

$\square$

Proof of Lemma 1: It is a direct conclusion of the definition of trace. Please see, for example, Formulae 4.13 (a) and (b) in Seber (2008). $\square$

Proof of Theorem 3: According to Theorem 2.3 and Table 2.1 in Fedorov and Leonov (2014), $\boldsymbol{\xi}$ is D-optimal if and only if $\max_{\mathbf{x} \in \mathcal{X}} d(\mathbf{x}, \boldsymbol{\xi}) \leq p$, where $d(\mathbf{x}, \boldsymbol{\xi}) = \mathrm{tr}(\mathbf{F}(\boldsymbol{\xi})^{-1}\mathbf{F}_{\mathbf{x}})$. Equation (3.2) can be obtained by applying Lemma 1 and Theorem 2, as well as

$$\mathrm{tr}(\mathbf{C}_{ij}u_{ij}^{\mathbf{x}}\mathbf{h}_i^{\mathbf{x}}(\mathbf{h}_j^{\mathbf{x}})^T) = u_{ij}^{\mathbf{x}}\mathrm{tr}((\mathbf{h}_j^{\mathbf{x}})^T\mathbf{C}_{ij}\mathbf{h}_i^{\mathbf{x}}) = u_{ij}^{\mathbf{x}}(\mathbf{h}_j^{\mathbf{x}})^T\mathbf{C}_{ij}\mathbf{h}_i^{\mathbf{x}}$$

$\square$

Proof of Theorem 4: For D-criterion, for example, see Fedorov and Leonov (2014, section 2.5), $\boldsymbol{\xi}$ is D-optimal if and only if

$$\max_{\mathbf{x} \in \mathcal{X}} \mathrm{tr}\left[(\mathbf{X}_{\boldsymbol{\xi}}^T\mathbf{W}_{\boldsymbol{\xi}}\mathbf{X}_{\boldsymbol{\xi}})^{-1} \cdot \nu(\boldsymbol{\beta}^T\mathbf{h}(\mathbf{x}))\mathbf{h}(\mathbf{x})\mathbf{h}(\mathbf{x})^T\right]$$

$$= \max_{\mathbf{x} \in \mathcal{X}} \nu(\boldsymbol{\beta}^T\mathbf{h}(\mathbf{x}))\mathbf{h}(\mathbf{x})^T(\mathbf{X}_{\boldsymbol{\xi}}^T\mathbf{W}_{\boldsymbol{\xi}}\mathbf{X}_{\boldsymbol{\xi}})^{-1}\mathbf{h}(\mathbf{x}) \leq p$$

S12

$\square$

Proof of Theorem 5: We are given the design at the tth iteration $\boldsymbol{\xi}_t = \{(\mathbf{x}_i^{(t)}, w_i^{(t)}), i = 1, \ldots, m_t\}$ and the new design point $\mathbf{x}^*$. We define a function of the allocation for the $(t+1)$th iteration $f^{(t)}(w_1, \ldots, w_{m_t+1}) = f(\{(\mathbf{x}_1^{(t)}, w_1), \ldots, (\mathbf{x}_{m_t}^{(t)}, w_{m_t}), (\mathbf{x}^*, w_{m_t+1})\})$.

Following the notations for the lift-one algorithm (see (1) in Yang and Mandal (2015)), we define $f_{m_t+1}^{(t)}(x) = f^{(t)}((1-x)w_1^{(t)}, \ldots, (1-x)w_{m_t}^{(t)}, x)$ for $0 \le x \le 1$. Then $f(\boldsymbol{\xi}_t) = f^{(t)}(w_1^{(t)}, \ldots, w_{m_t}^{(t)}, 0) = f_{m_t+1}^{(t)}(0)$. According to Lemma 4.1 in Yang and Mandal (2015), $f_{m_t+1}^{(t)}(x) = ax(1-x)^{p-1} + b(1-x)^p$ with $b = f(\boldsymbol{\xi}_t) \overset{\triangle}{=} b_t$ and $a = f_{m_t+1}^{(t)}(1/2) \cdot 2^p - b \overset{\triangle}{=} d_t \cdot 2^p - b_t$. The conclusion then can be drawn from Lemma 4.2 in Yang and Mandal (2015). $\square$

Proof of Theorem 6: $\mathbf{X}_{\boldsymbol{\xi}} = (\mathbf{h}(\mathbf{x}_1), \ldots, \mathbf{h}(\mathbf{x}_m))^T$ is $m \times p$, $\mathbf{W}_{\boldsymbol{\xi}} = \mathrm{diag}\{w_1\nu(\boldsymbol{\beta}^T\mathbf{h}(\mathbf{x}_1)), \ldots, w_m\nu(\boldsymbol{\beta}^T\mathbf{h}(\mathbf{x}_m))\}$ is $m \times m$, and $\mathbf{X}_{\boldsymbol{\xi}}^T\mathbf{W}_{\boldsymbol{\xi}}\mathbf{X}_{\boldsymbol{\xi}}$ is $p \times p$. Then $f(\boldsymbol{\xi}) > 0$ implies $p = \mathrm{rank}(\mathbf{X}_{\boldsymbol{\xi}}^T\mathbf{W}_{\boldsymbol{\xi}}\mathbf{X}_{\boldsymbol{\xi}}) \le \min\{m, \mathrm{rank}(\mathbf{X}_{\boldsymbol{\xi}})\}$. That is, $\mathrm{rank}(\mathbf{X}_{\boldsymbol{\xi}}) = p \le m$. If furthermore, $\nu(\boldsymbol{\beta}^T\mathbf{h}(\mathbf{x}_i)) > 0$ for all $i = 1, \ldots, m$, that is, $\mathbf{W}_{\boldsymbol{\xi}}$ is of full rank, then $\mathrm{rank}(\mathbf{X}_{\boldsymbol{\xi}}^T\mathbf{W}_{\boldsymbol{\xi}}\mathbf{X}_{\boldsymbol{\xi}}) = \mathrm{rank}(\mathbf{X}_{\boldsymbol{\xi}})$. Therefore, $f(\boldsymbol{\xi}) > 0$ if and only if $\mathrm{rank}(\mathbf{X}_{\boldsymbol{\xi}}) = p$. $\square$

Proof of Theorem 7: In this case, $m = p$, $\mathbf{X}_{\boldsymbol{\xi}}$ is $p \times p$, and $f(\boldsymbol{\xi}) = |\mathbf{X}_{\boldsymbol{\xi}}^T\mathbf{W}_{\boldsymbol{\xi}}\mathbf{X}_{\boldsymbol{\xi}}| = |\mathbf{X}_{\boldsymbol{\xi}}|^2 \cdot |\mathbf{W}_{\boldsymbol{\xi}}| = |\mathbf{X}_{\boldsymbol{\xi}}|^2 \prod_{i=1}^{p} \nu(\boldsymbol{\beta}^T\mathbf{h}(\mathbf{x}_i)) \cdot \prod_{i=1}^{p} w_i$. Since $\prod_{i=1}^{p} w_i \le p^{-p}$ with equality attaining at $w_i = p^{-1}$, then $\boldsymbol{\xi}$ is D-optimal only if $w_i = p^{-1}$, $i = 1, \ldots, p$. $\square$